Icarus 378 (2022) 114941

Contents lists available at ScienceDirect

Icarus

journal homepage: www.elsevier.com/locate/icarus

Wind-snow interactions at the Ojos del Salado region as a potential Mars analogue site in the Altiplano - Atacama desert region

A. Kereszturi [a,j,*], J.M. Aszalos [b], Heiling Zs [c], Á. Igneczi [i], Kapui Zs [d], Kiraly Cs [e], Leel-Ossy Sz [f], Z. Szalai [e,h], Nemerkenyi Zs [e], B. Pal [a], A. Skulteti [e], B. Nagy [g]

[a] Konkoly Thege Miklos Astronomical Institute, Research Centre for Astronomy and Earth Sciences, H-1121 Konkoly-Thege Miklos 15-17, Budapest, Hungary
[b] Department of Microbiology, Eötvös Loránd University, 1117 Budapest, Pázmány Péter 1/C, Hungary
[c] Földgömb Foundation for Research Expeditions, H-1142 Budapest, Erzsébet királyné útja 125, Hungary
[d] Research Centre for Astronomy and Earth Sciences, Institute for Geological and Geochemical Research, H-1112 Budapest, Budaörsi út 45, Hungary
[e] Geographical Institute, Research Centre for Astronomy and Earth Sciences, H-1112 Budapest, Budaörsi út 45, Hungary
[f] Department of Physical and Applied Geology, ELTE Eötvös Loránd University, 1117 Budapest, Pázmány Péter 1/C, Hungary
[g] Department of Physical Geography, ELTE Eötvös Loránd University, 1117 Budapest, Pázmány Péter 1/C, Hungary
[h] Department of Environmental and Landscape Geography, Eötvös Loránd University, H-1117 Budapest, Pázmány Péter 1/C, Hungary
[i] Department of Geography, University of Sheffield, Winter Street, Sheffield, S3 7ND, UK
[j] European Astrobiology Institute, Strasbourg, France

ARTICLE INFO

Keywords:
Mars
Analogue
Field site
Cryosphere

ABSTRACT

We describe the general characteristics and interactions happening at a unique, potential new Mars analogue site, located in the Altiplano and Atacama Desert region: the Ojos del Salado inactive volcano. The interaction between rare snowing events and strong winds transported large masses of porous volcanic grains there could produce decimeter - meter thick buried snow masses fast, shielded against sublimation for extended periods (years). Subsurface temperature logging suggests that water ice melting is rare and surface modification is dominated by desiccation of the cryosphere and wind activity – just like on Mars. The first analysis of aeolian transported grains in the area points to immature material sized between coarse sand and coarse silt, and indicates the possibility of larger snow occurrence in winter when the site is inaccessible – however further observations are necessary The site contains decameter scale megaripples, which are unusual for Earth and also support the understanding of resemble features on Mars. The shallow subsurface analysis with Mars relevance is supported here by drilled cores of evaporitic sediments presented carbonate, aragonite, anhydrite, talc and clay minerals in the shallow subsurface with Mars relevance. Though the region is generally felsic in composition, basalts can be found at a hillside near Laguna Verde where the effect of extreme conditions (including the strong UV radiation) on rock weathering could be analysed. The temperature, dryness, wind exposure, decreased atmospheric pressure and elevated UV radiation together make Ojos del Salado a unique Mars analogue site, and it is accessible up to 5200 m altitude by regular pick-up trucks via a 5–6 h driving from the Copiapo airport.

1. Introduction

Field analysis at Mars analogue terrains targeting extreme locations on our planet supports the understanding of processes and surface features of Mars. The aim of this paper is to give a general overview of the high altitude desert area at Ojos del Salado (Fig. 1) focusing on the following main questions: How the ephemeral snow produces melting and runoff, how surface features reflect the characteristics of the permafrost at a dry terrain – and in general what are those analogue aspects that could be more effectively analysed here than at other sites on the Earth.

Ojos del Salado emerged as a potential Mars analogue recently (Kereszturi et al., 2020a, 2020b), where a range of analogue aspects could be addressed, which were also studied at other sites recently, including post-volcanic aspects (Mege et al., 2018), volcanic rock mineralogy (Gurgurewicz et al., 2015), geomorphology and grain

* Corresponding author at: Konkoly Thege Miklos Astronomical Institute, Research Centre for Astronomy and Earth Sciences, H-1121 Konkoly-Thege Miklos 15-17, Budapest, Hungary.
E-mail address: kereszturi.akos@csfk.org (A. Kereszturi).

https://doi.org/10.1016/j.icarus.2022.114941
Received 11 November 2020; Received in revised form 6 February 2022; Accepted 8 February 2022
Available online 14 February 2022

transport of desert areas (Ori et al., 2014), surface water runoff (Grau Galofre et al., 2020; Ettahri and Hargitai, 2020, Wilcox et al., 2016), surface and subsurface ice occurrence (Cousins et al., 2013; Douglas and Mellon, 2019; Gourronc et al., 2014; Pandey et al., 2020), and meteorological aspects (Weidinger et al., 2009). Several expectations can be addressed based on the probable conditions at this extreme site, including the dryness, low temperature by the high elevation, where even rare precipitation events might have important consequences. Connected to these aspects, permafrost might emerge in the region, and due to the general dryness, sublimation could have a stronger role than melting. The poorly consolidated volcanoclastic debris on the surface moved by the strong winds are expected to produce a moderately active environment, probably just like on Mars. These possibilities and the related research questions emerged to better understand the properties of the area.

This site contains extreme habitats supported by ephemeral ice melting and volcanic heat related liquid water production at a dry and strongly UV radiation exposed area. The UV irradiation increases along with the elevation by the decreasing amounts of air above, including ozone, aerosols and clouds. While UV-C is screened above about 20–30 km, UV-B and -A could reach the analysed elevation range. The total irradiance at the Atacama Base Camp about 5200 m elevation is estimated to be about 176–178% of those at sea level in the case of a cloudless sky (Blumthaler et al., 1997; Chubarova et al., 2016; Schmucki

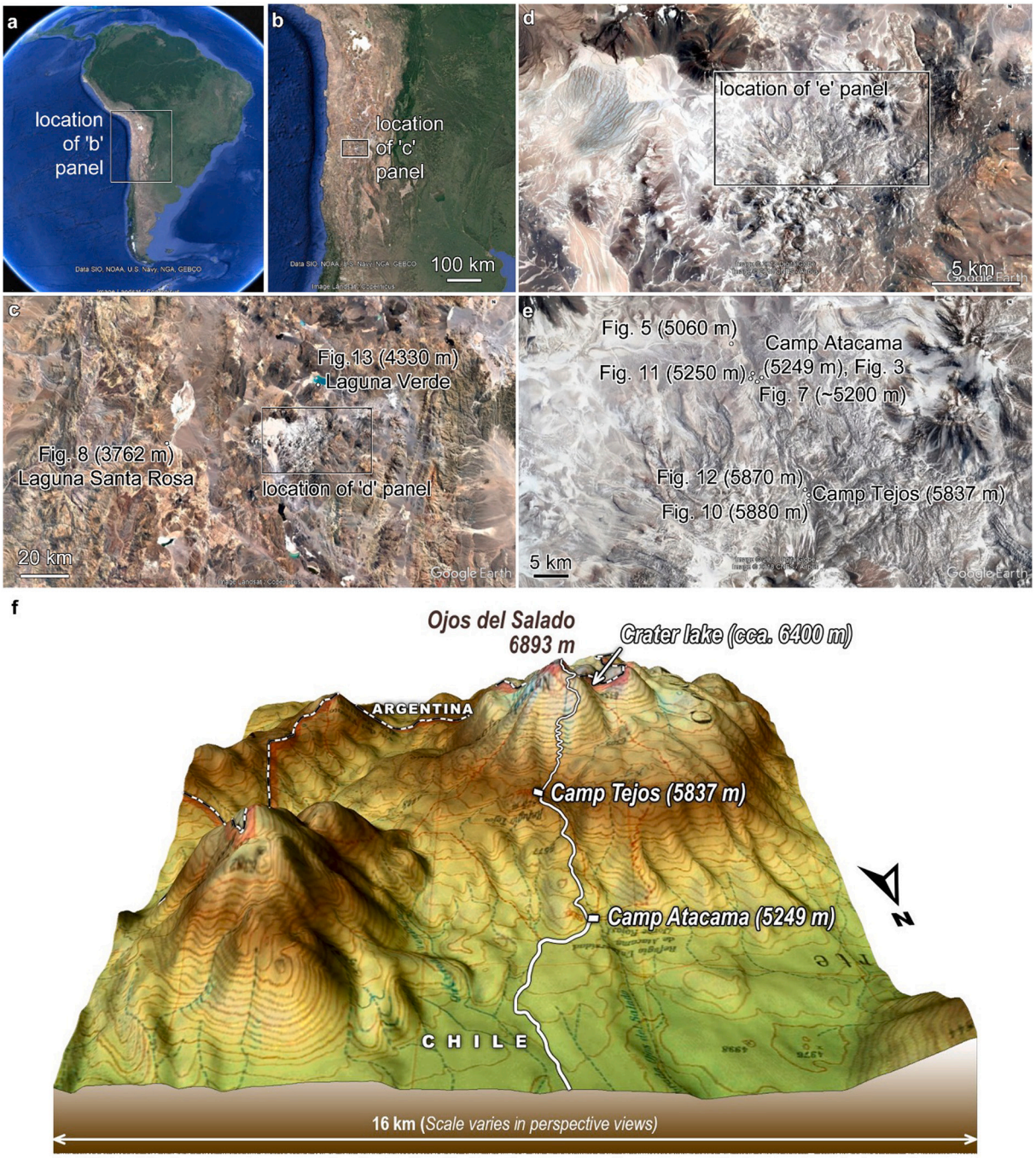

Fig. 1. Overview of the Ojos del Salado region: a: wider area of Southern-America, b: the north-south range of the Andes Mountain, c: smaller area of the Altiplano and Atacama Desert region, d: the targeted Ojos del Salado region, e: the northern slopes of the volcano (GoogleMaps images), f: perspective view of the target area. North is upward in all insets, except the last one (f) where specifically indicated. The locations of some panels are indicated in 'c' and 'e' panels.

and Philipona, 2002). On Mars the total integrated flux in the UV-A range is roughly comparable to those on the Earth, however shorter wavelength (UV-B, UV-C) is much stronger (Cockell, 2002). Although the above mentioned parameters are not as extreme as on Mars, the processes acting on the cryosphere, the interaction between ephemeral snowing (partly analogous for those observed at the landing site of Phoenix on Mars, Spiga et al., 2017) and wind transported material are Mars relevant. The knowledge on the geological context helps to better estimate the conditions on Mars and improve the methods to analyse the astrobiology aspects of the red planet.

Interacting topics are presented and arranged to order of logical connections in this work: starting from meteorological conditions, followed by aeolian features and survey of wind transported grains, describing rare precipitation and strong wind driven surface change monitoring, until the shallow subsurface analysis and found evaporates in the area. These topics help to understand the connections and interactions between the different factors and also to see the whole potential of this site. Some of these results are only preliminary one, but could be interesting for the community as they offer insight to the opportunities provided by this analogue site. In addition to this general overview, some specific examples of various analysis types are also presented here, in order to offer more details on the local conditions and provide examples of the variety of results, what may be possible to acquire in the future.

1.1. General information on the site

This analogue research work was realized at the Ojos del Salado (6893 m, 27°06′34″ S, 68°32′32″ W), in the Atacama-Altiplano region, which is the highest volcano on Earth (Óscar, 1995) with an elevation of 6893 m. The volcano started its activity around 26 Ma (million years) ago (Mpodozis et al., 1996), producing gradually evolved geochemistry (DeSilva and Francis, 1991) toward acidic compositions (Bakero et al., 1987), until about 30 kyr ago (Moreno and Gibbons, 2007). Today only fumarolic activity could be observed. This region is a desert without vegetation and soil, with several salty lakes or their dried up deposits. At high altitude permafrost is present (Ahumada, 2002; Cobos and Corte, 1990) with glacier remnants (Oyarzun, 1987), and the surface is dominated by rocks and boulders, with rare ripples and dunes. The highest altitude snowline on Earfth is present here (Clapperton, 1994), above 6500 m the terrain is mostly snow covered (Ammann et al., 2001), the highest altitude lakes are also present here on Earth. Stochastic changes and the poor observational coverage makes the characterization of the local climate uncertain. The nighttime temperatures can drop below −10 C even during summertime at the elevation of the Atacama Base camp, while above 6000 m it is often below −10 C even in daytime. High altitude desert conditions are present below 6000 m in the region (Azócar and Brenning, 2010; Ammann et al., 2001; Houston and Hartley, 2003; Nagy et al., 2014a, 2014b; Nagy et al., 2019; Vuille and Ammann, 1997). Precipitation as snow occurs but rarely here (no rain above 5000 m altitude), mainly during local winter (May–October). It might sublimate away in most cases, but partly can be stored for later melting and runoff (see Kereszturi, 2020).

No glaciers are present at the time of writing, but several were present in the past (Nagy et al., 2019) about 19 ka ago (Ammann et al., 2001). Permafrost exists as patches above 5200 m, and continuously above 5600 m (Nagy et al., 2019). The annual precipitation is around 20 mm/year, however highly variable from year to year. Long-term cryosphere monitoring started in 2012 by installing loggers at 5 different altitudes (see further details in Nagy et al., 2019).

1.2. Analogue work at Atacama and Altiplano

Mars analogue sites on Earth has provided a range of Mars relevant information on various geological features (Preston et al., 2012; Schwendner et al., 2018), geological history (Hauber et al., 2011), and potential biological aspects (Azua-Bustos et al., 2012; Warren-Rhodes et al., 2018). These locations also provide possibility to realize tests for mission instruments (Groemer et al., 2016; Ross et al., 2013; Thirsk et al., 2007). Ojos del Salado is unique among the other analogue sites in certain ways, which are discussed in this work.

The Altiplano and Atacama regions has already been considered as a Mars analogue regarding their general dryness (McKay et al., 2003), microbiological aspects (Azua-Bustos et al., 2015), specific runoff and valley network development (Harrison and Grimm, 2005; Irwin et al., 2014), gully formation (Heldmann et al., 2010) and flood events (Wilcox et al., 2016). Several astrobiology relevant projects have been realized here, including the possibility of soil development (Ewing et al., 2006; Sutter et al., 2007), evaluating the UV screening effect of soils (Ertem et al., 2017), spectral characteristics of evaporites at salars (Flahaut et al., 2017), soil organic turnover (Ewing et al., 2008), perchlorates related surface chemistry (Catling et al., 2010) and the role of halite in organic preservation (Fernández-Remolar et al., 2013). At the driest locations nitrate and perchlorate accumulation could happen (McKay and Claire, 2016), where primary production occurs inside hygroscopic halite crusts (Wierzchos et al., 2009). Water acquisition is based on fogs here by deliquescence on hygroscopic crystal surfaces (Davila et al., 2010). Microscale temperature measurements with high sampling intervals suggests that strong temperature variation could contribute to rock weathering (McKay et al., 2009) there.

Mapping the regional distribution of life and potential habitats along with the increasing dryness was completed in order to identify the ideal payload for a rover to survey for microbial life signatures (Cabrol et al., 2007) by fluorescence signals, characterizing local geology by imaging and spectral analysis, and to evaluate various mission strategies (Cabrol et al., 2001). The results were correlated to space based remote image analysis (Piatek et al., 2007; Warren-Rhodes et al., 2007), and supported the development of a habitat related scoring system (Hock et al., 2007). Ignimbrite as a potential habitat has been also surveyed in the region (Wierzchos et al., 2013), including its potential as a specific water source (Wierzchos et al., 2012), targeted pH and redox potential analysis, plus ion concentration measurements as well as carbon and amino acid abundances of soils (Peeters et al., 2009). Field testing of the SAM instrument onboard Curiosity rover (Stalport et al., 2012), organics detection (Blanco et al., 2013), testing the Life Detector Chip (Parro et al., 2011), Raman method for rock analysis (Vitek et al., 2014), and satellite-rover synergic habitat mapping (Warren-Rhodes et al., 2007) were realized in the region, just like the analysis of science autonomy (Smith et al., 2007). Several field tests and developments were done like testing the TEGA instrument of Phoenix lander (Valdivia-Silva et al., 2009) or LIBS for Curiosity rover (Sobron et al., 2013). Beside the above listed topics, the examination of a rover mounted drill (Cabrol et al., 2014) and strategies for robotic exploration related to astrobiology in general (Hock et al., 2007) were done. Organic material and water extraction were also tested (Amashukeli et al., 2008), and microhabitats (Schulze-Makuch et al., 2018), especially inside halite have been analysed here (Wierzchos et al., 2012). The search for biosignatures in the Yungay region (driest part of the Atacama Desert) provided desiccation-tolerant organisms (Boy et al., 2017; Skelley et al., 2007), and a range of salt tolerant ones (Davila et al., 2010; Wierzchos et al., 2006). Strongly UV irradiated microhabitats have also been identified in Sairecabur volcano at 5971 m (Pulschen et al., 2015) nearby.

1.3. Specific Mars analogue aspects of Ojos del Salado

The research work at the Ojos del Salado region started in 2012, focusing on the analysis of the shallow subsurface temperature regime and the occurrence of permafrost. The aim was to monitor and forecast the aftereffects of global warming related permafrost degradation, together with the survey of potential consequences on the accessible liquid water there. The Ojos del Salado region shows several characteristics, which contribute to Mars relevant processes, though that the

numerical conditions are not as extreme on Mars. The low temperatures (yearly average of 0.02 °C at 5200 m elevation as measured by own instruments from the 2014–2016 period) are accompanied with dryness (Kereszturi et al., 2020a, 2020b). The lowest measured temperature was −25 °C. Nightly frost could form even during the summer but sublimates easily daytime under the large daily temperature fluctuations (>20 °C). This might have unique consequence on weathering because the regolith is usually dry. Other unique aspects are the rare precipitation that allows to analyse how ephemeral snow could be retained by shallow burial. The permafrost that exists at a dry terrain and degrades, the generally strong winds, lack of vegetation, the general slow weathering, erodible volcanic material and elevated UV irradiation are providing Mars relevant aspects.

The diagram in Fig. 2. helps to compare the temperature and precipitation values of this site to other locations. The following temperature vales were measured at 6000 m above sea level on Ojos del Salado: Unfortunately the precipitation values are highly uncertain at Ojos del Salado, but it is still obvious that these parameters are much more elevated than those characteristic for Mars. Although no directly measured data is available there, the values extrapolated from measurements in the wider region point to that mean annual rainfall between 1977 and 2000 was around 20 mm/year (highly variable, Houston, 2006). Calculating related error bar is not much relevant here, as its size is larger than the 20 mm average in positive direction, with no precipitation at all in certain years. Despite that snow accumulation could be observed occasionally, its inhomogeneous spatial distribution produced by the wind inhibits to use the snow thickness for precipitation estimation.

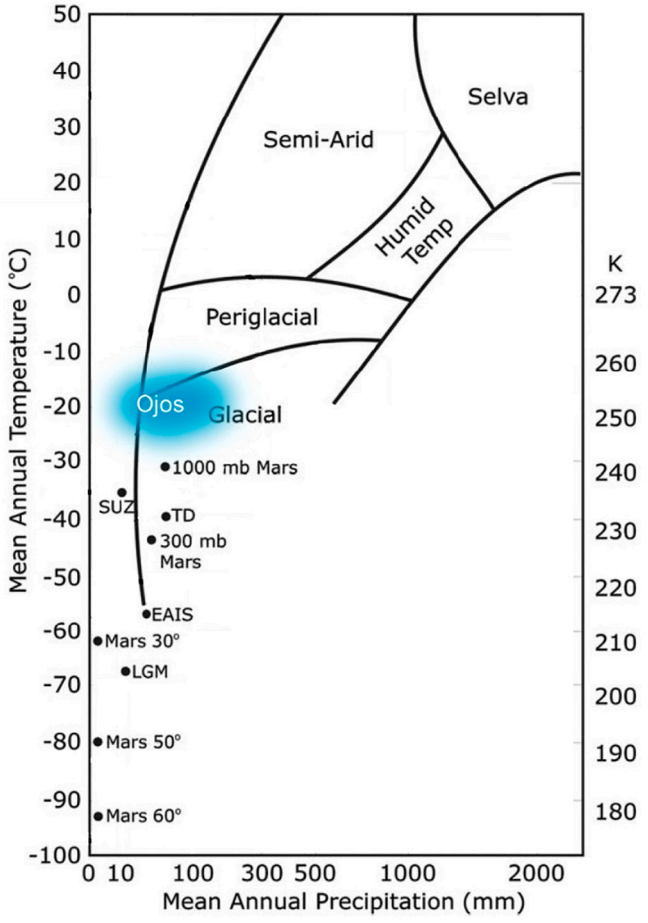

Fig. 2. Mean annual temperature versus precipitation at certain characteristic locations on Earth and Mars (adapted from Baker, 2001, Marchant and Head, 2007 and Levy et al., 2011). Modern Martian conditions are indicated by "Mars" and the value of latitudes after that: 30°, 50°, and 60°. The roughly estimated ancient conditions on Mars at 300 and 1000 mbar pressure atmospheres are also indicated. The "Ojos" text marks the analysed area in this work, mainly around 5800 m elevation. Further acronyms: Antarctic Dry Valleys stable upland zone (SUZ), modern conditions at Taylor Dome (TD), 35 km south-west of the Antarctic Dry Valleys, while current conditions at Vostok interior of East Antarctica (78° S) marked by EAIS. LGM is for the conditions during the last glacial maximum (~18 ka) in the interior East Antarctica.

2. Methods

The acquired information on this site came mainly from fieldwork (imaging, digging, on-site sedimentary analysis), including the use of various temperature data loggers that could run for several years. These were HOBO Pro v2 waterproof loggers with 12-bit resolution (operation range: −40 °C to +70 °C, accuracy ±0.21 °C) at multiple depths (10, 20, 35, 60 cm). Shallow ground temperatures were registered hourly and the loggers were read out using USB connection in every second years. The information gained in the field were completed with remote sensing based images and topographic datasets. The range of the outcomes presented here provide examples on how various disciplines could support synergistic results at this Mars analogue site.

Aeolian grain collecting was done at three locations using wind traps (Fig. 3). At all locations the traps were composed of 5 similar 25 cm wide, 10 cm high and 15 cm deep, pocket shaped material made of UV resistant geotextile (called pockets hereafter), located above each other. The first trap covered 0–10 cm, the second 10–20 cm height and so on, up to the fifth trap about 40–50 cm above the ground. Three of such vertically arranged trap systems were installed between 2016 and 2018 at the following altitudes: SZ-1 at 5230 m elevation, SZ-25260 m (both close to the Atacama base camp, located around 250 m from each other), the SZ-3 at 6000 m (close to the Tejos camp located at 27°05′14″S 68°32′17″W). During grain size measurements Wentworth scale was applied.

The grains collected from the trap were engulfed by a plastic bag at their location, unattached them from the holding frame and shake to the plastic bag to fall all grains into it from the given trap. The acquired grains were analysed by Malvern Morphologi G3 ID, a high-resolution analytical instrument, that was used in the laboratory for the shape analysis of large (>10,000) number of grains with a built-in statistical software, that yielded relevant morphometric parameters. The dispersed grains were scanned and the morphometrical parameters were determined. Histograms were created to represent this data, and also to select specific groups for more detailed analysis. The instrument is capable of providing various statistical parameters of the grains, including diameter, length, width, perimeter, major axis, area, volume, circularity, convexity, aspect ratio and elongation for particles. The measurement covers the size range of 1–1000 μm with a spatial resolution of optical data 1 μm.

At some locations drilled holes for sample cores by hand forced simple cylindrical auger was acquired. The results presented in the 3.5 section are based on two methods. 1. The material acquired at Laguna Santa Rosa indicated in Fig. 1 c inset, of the lower part of the borehole (not influenced by recent surface wind and evaporation driven drying effects at the surface) was analysed for mineral determination in the home laboratory with Fourier Transformational Infrared Spectroscopy using Vertex 70 FTIR spectrometer, Attenuated Total Reflectance (ATR) method. During the infrared analysis of the minerals, the sample was in contact with the tip of a germanium (Ge) crystal, 100 μm in diameter. All measurements were performed for 30 s at 4 cm^{-1} spectral resolution and Bruker Optics' Opus 5.5 software was used for manipulation of the recorded spectra.

3. Results

This section was structured to provide an overview of the interacting

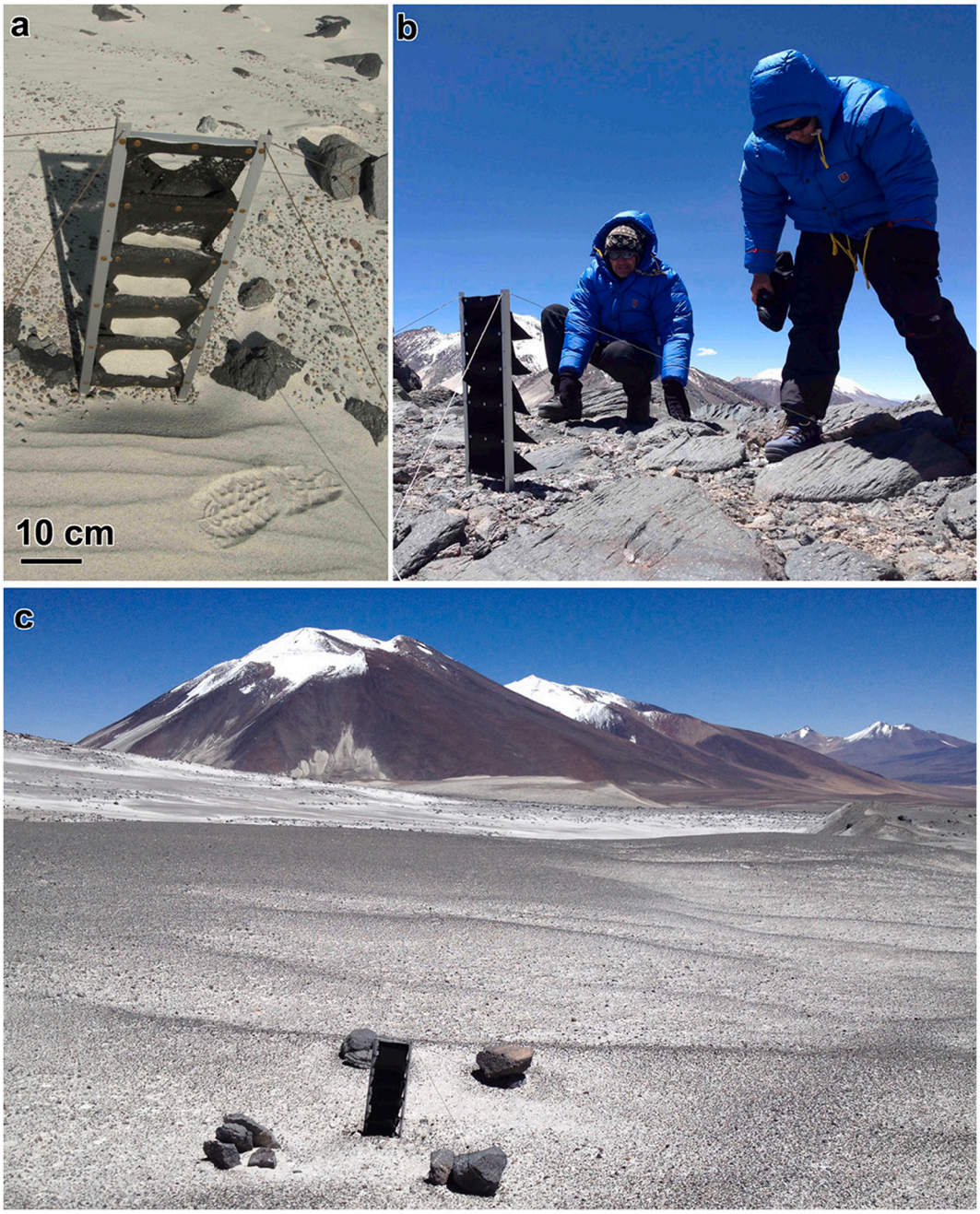

Fig. 3. Image of one wind trap (a, SZ-1) filled with grains, together with its surroundings (b, SZ-3) and (c, SZ-2). Please note for scale the width of the wind traps are 25 cm.

aspects observable at this site, starting with the general temperature and humidity characteristics, then and aeolian grain analysis wind produced surface structures, followed by surface change monitoring, finished by shallow subsurface characteristics of evaporates, and the occurrence of subsurface ice. These topics are presented in order to give specific insight into the conditions and targets at the site.

3.1. Temperature and humidity cycle

The characteristic annual temperatures for the area are visible in Fig. 4 inset 'a' and 'b'. The annual trend is correlated with the solar illumination changes, with the warmest summertime period with +6 … +10 °C around January, when the daily temperature fluctuation is also the highest. This is supported by the dry condition and the porous material that caused low thermal inertia of the surface covering, what allows fast warming in daytime and also effective cooling in nighttime. In wintertime the daily maximum temperature ranges around zero Celsius. To provide a wider context for the interpretation of H_2O occurrence related observations at the site, temperature and relative humidity monitoring were also realized. The two curves in Fig. 4 'c' an 'd' insets demonstrate the daily temperature and humidity changes at the Laguna Verde (4300 m) and at the Atacama base camp (6200 m) sites on the days 17 and 20 of February 2018 respectively. It is visible that the two curves follow opposite trends and while in daytime the humidity is very low (30–35% at 4300 m elevation, 15–18% at 6200 m elevation), in night time it could be close to saturation due to the low temperature. The "mirrored appearance" of temperature and humidity curves is stronger at Fig. 4 c than 4 d, as the elevation of 4 c at the Atacama Basecamp is larger than the 4 d at Laguna Verde. At higher elevation the warming and cooling is faster possibly because of the

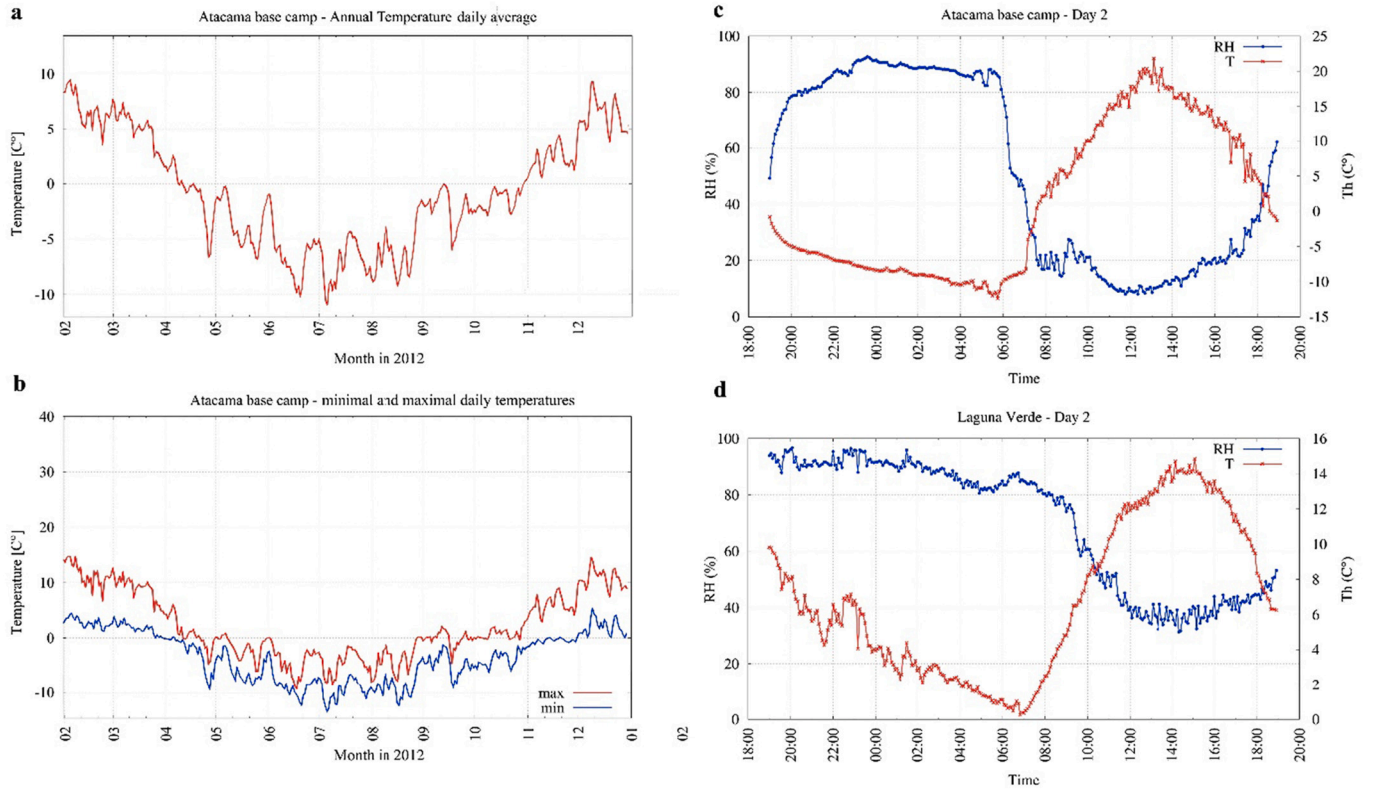

Fig. 4. Annual temperature curves a – daily average, b – min. and max. curves, c and d – temperature and relative humidity curves for the Atacama base camp and the Laguna Verde respectively.

thinner air mass above it and the dryer surface material.

The mirrored shape of the temperature and relative humidity curves was already expected. The daily temperature variation is somewhat above 30 °C at the more elevated location, where close to saturation conditions are present at night, while daytime RH approaches only 10%. These aspects are partly similar to Mars, where saturation or even oversaturation might emerge in nighttime at much lower absolute humidity. This is because of the even lower nighttime temperatures (Martin-Torres et al., 2015) providing a possibility for H_2O condensation and the emergence of microscopic liquid water on Mars despite the very low absolute vapour content.

3.2. *Aeolian features and transported grain observations*

Wind ripples can be observed in the region (Fig. 5). On Earth these features are cm-spaced usually, here they are larger and coarser mainly at the luv (wind shadowed) side of the hillslopes and on the plains, which usually show larger sizes above 4–5 km altitude (Milana, 2009). Their height is in the range of 2–230 cm, while the peak to peak distance ranges from 1 to 44 m. At the surveyed area around the Atacama Basecamp, the ripples were present in roughly 100–200 m diameter patches (see some examples in Fig. 5 panel 'e'). They are composed mostly of bright pumice grains and sand sized fraction with porous structure and density around 0.8–1.1 g/cm^3. A specific feature at several locations is that darker and higher density grains (2.5–3.0 g/cm^3) are present at the top of the ripples, thus on the top of smaller density grains (see inset 'c' in Fig. 5). Similar ripples can be found up to 1500 years old in Argentina at 4400 m elevation with similar composition and geological settings (Bridges et al., 2012; Nagy et al., 2019). At the Argentean Puna area gravel mantled megaripples were identified in the region (Bridges et al., 2015), where vibration of clasts and infiltration of small grain size downward found to be a strong agent in their formation, supported by laboratory tests. Based on the cited works including Sullivan et al., 2014, the observed features discussed here should be termed as megaripples hereafter (Chojnacki et al., 2021). The importance of the aeolian feature analysis (including their stratigraphy) is that temporal evolution could be monitored in an active environment, and the grains could also be surveyed regarding size, composition and morphology. (For the overview of the related information on Mars see the corresponding part of the Discussion section.)

The wind transported grains were collected in three sets of aeolian collectors at three different locations, two at 5230 m elevation (Atacama base camp), with about 250 m distance between them (SZ-1, SZ-2), and the third at 6000 m elevation near to the Tejos camp (SZ3). All locations were wind exposed sites, e.g. no topographic obstacles taller than 20–30 cm could be found closer than 6–8 m distance from the collectors, thus the wind could blow relatively free at the locations of the traps.

In each trap a large mass of aeolian material was accumulated during the 2016–2018 interval (meaning that the total volume of the traps were filled by aeolian transported debris, see specific numbers in the Fig. 6 for each trap), except some collector pockets of the SZ-3 trap (the one situated at 6000 m elevation), where the geotextile of these collectors was frozen and did not keep the pocked shape, thus was not able to collect grains. The mass of the collected grains in most of the traps ranged between 100 and 200 g, with three obvious exceptions: range 0.4–0.6 g values for SZ-1/5, SZ-3/1 and SZ-3/3. The samples for detailed analysis were randomly selected from the mixed collected grains for each trap. In these cases the curves differ from the rest of the samples, they showed the most populated peak at coarse sand around 1000 μm (Fig. 6). For detailed numerical data on the collected samples see Table SOM. A weaker second maximum or shoulder appeared around 700–900 μm. No obvious trend was observed between the number or mass of collected grains and the height of the given trap – except at these high located pockets, see below.

In the trap SZ-1/5 (5th i.e. highest pocket above the ground) larger grains (700–1200 μm) were more frequent than in its lower situated

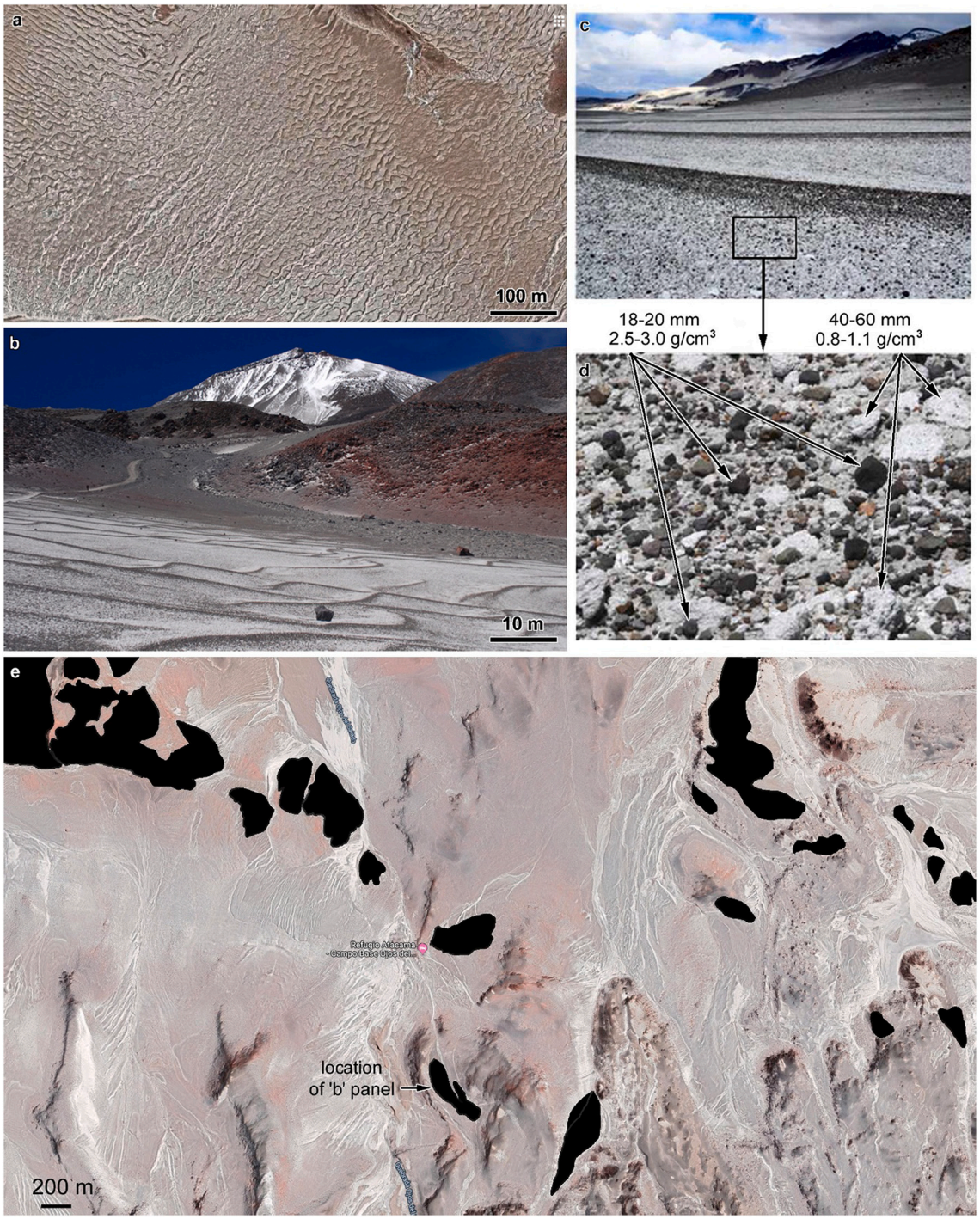

Fig. 5. Wind ripples from above (a) and sideward (b) near to the Atacama base camp around 5200 m elevation. Insets 'c' and 'd' show the locations of different grains nearby, and 'e' the spatial occurrence of the ripple groups in the region.

pockets. In the case of SZ-3 trap, the useful pockets (number 1 and 3) also show a similar trend, where larger grains are more frequent than in most cases (grains below 62 μm diameter e.g. coarse silt is usually <4%), and in trap 3 dominates (the largest ratio values for SZ-1/5, SZ-3/1 and SZ-3/3 are >6%. In the case of SZ-2 traps, the highest pocket (5) also shows a somewhat elevated occurrence of this larger size domain (800–1200 μm, coarse or very coarse sand), but not as much as the above mentioned cases. From fine to coarse sand fractions are abundant in the samples, the circularity is relatively large (0.8–0.9) but the grains are not smoothly rounded and they show undulating surface with many idiomorph and euhedral shapes (Fig. 6 top right panel with grain silhouettes). Altogether these observations point to that at larger elevations above the ground in SZ-1 and -2 a higher ratio of larger grains might be present. No known process during the sample handling could produce such result (artefact) – thus the unusual size distribution is real. No grains smaller than very fine sand could be observed, which was not the result of sample handling, as during the sample acquisition from the pockets, all the grains were enveloped in a plastic bag. For comparison three images of wind transported material are visible in the top right part of Fig. 6 as separated grains. Below them three vertical image stripes are presented from Mars for comparison, only to see in context with grains there. Left: grains at Gobabeb (Otavi target), middle: ripple

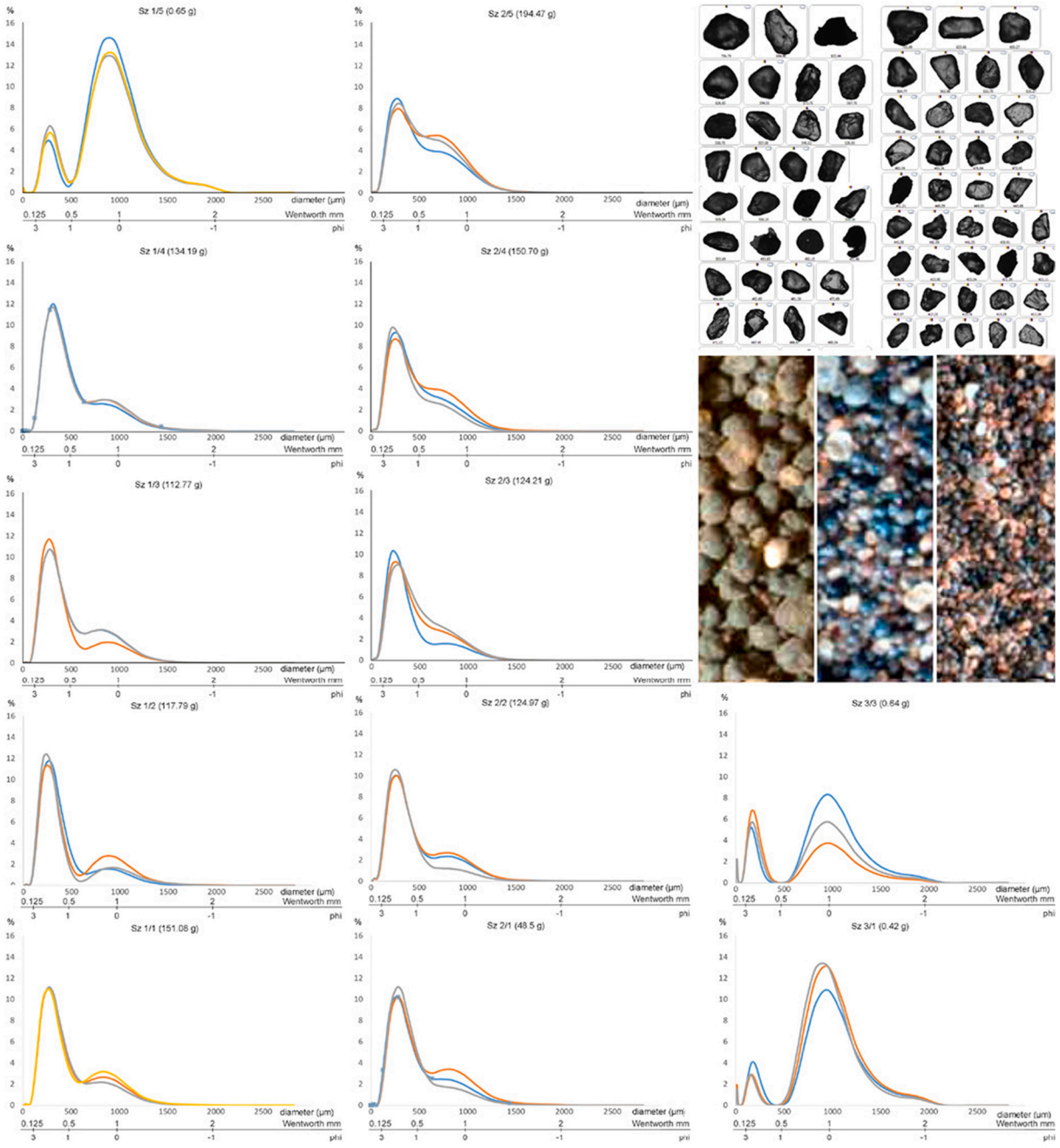

Fig. 6. Grain size distribution curves of the wind traps acquired samples. The trap id. number is visible above each diagram (SZ-1 first column, SZ-2 s column, SZ-3 third column, traps are arranged upward according to increasing number and height on site), and the acquired mass of the given trap can be read here in bracket. The top right inset shows example high resolution images of the grains larger than 1 mm, with many idiomorph and euhedral shapes. The three curves in each diagram show three different measured samples acquired of the same trap. The similarity of each diagram shows that the given measurement is representative for the given trap.

crest of Mapleton (Flume Ridge target) and right: Enchanted Island target, all recorded by MAHLI on-board Curiosity rover (Lapotre et al., 2018).

3.3. Surface change monitoring

Over the course of nearly ten years, a series of images were recorded of the same surface areas in order to identify the potential changes possibly related to the strong wind and the rare snowing events. Some examples of such changes are presented in Fig. 7, recorded in 2012, 2014, 2016 and 2018. The depressions observable in 2012 were partly filled in 2014, and totally filled in 2016, while the valley of a stream was eroded and exposed large volume in 2018. The two small insets at the bottom right show the same large (meter sized) block that slumped down between 2016 and 2018 on the slope.

Comparing the images of the same area recorded at different years (Fig. 7), the following modifications were identified: surface changes are obvious in the areal distribution of bright dust, silt, sand and pumice; substantially modifying the appearance (mainly the albedo) of a given location, even though it influences only a thin surface layer. Depressions (usually shallower than 1 m) could be filled by sediments (sand, pumice and occasionally snow) creating a smoother topography. These infilled

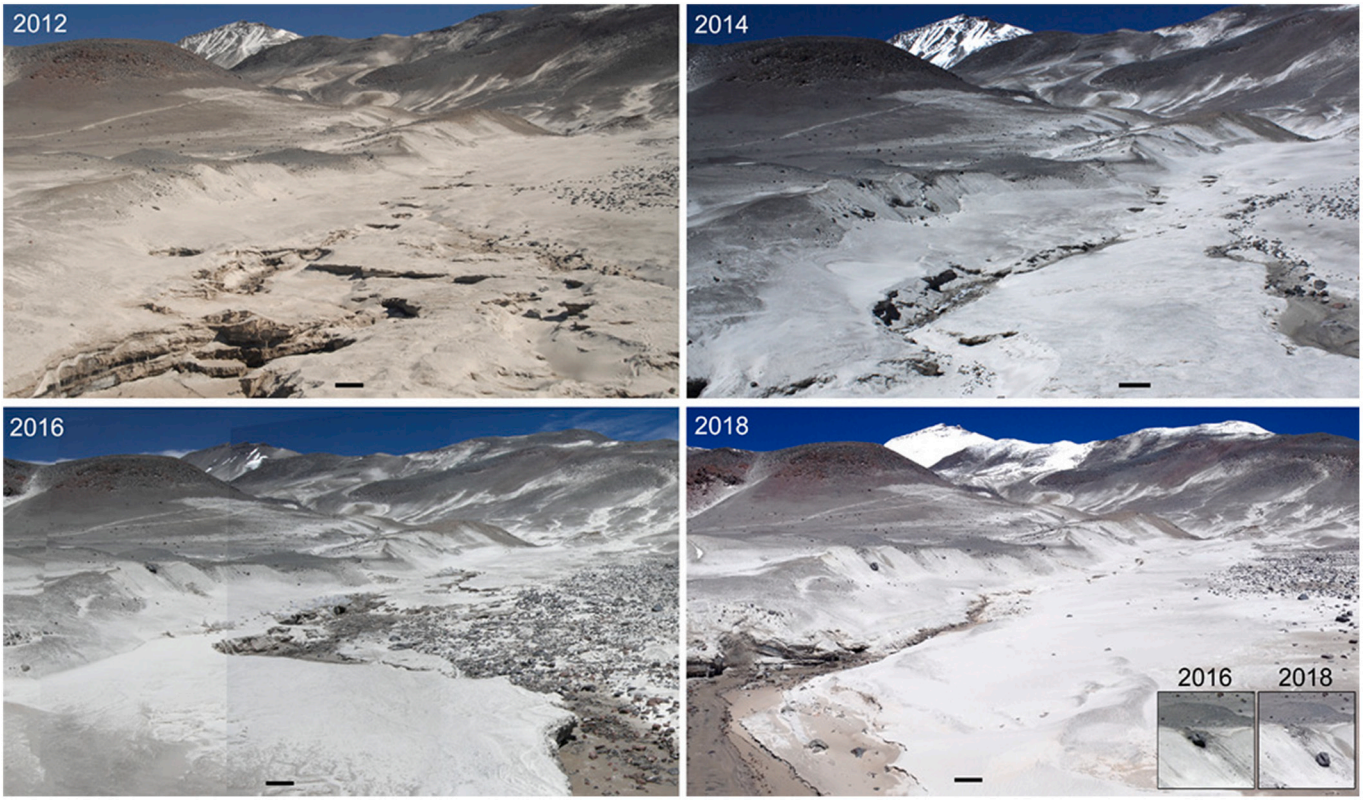

Fig. 7. Surface changes between 2012 and 2018 at the same area. The black bars at the bottom mark 1 m size at the foreground of the images. The two small insets at the lower right show magnified the slumped block in 2016 and 2018. Please note the filled depressions in the foreground (bottom left) from 2014 to 2016, which were partly "re-exhumed" in 2018. All these images were recorded during local summer (January and February when the site is easily and safely accessible).

areas and depressions could be eroded and exhumed subsequently.

The appearance of the spatial distribution of rock blocks changed because the dust, sand and pumice filled in the area between them, as the sedimentation or erosion of deposits could change the elevation of the local surface by mm-cm scale, covering or exposing the rocks already situated there. Though observed only in few cases, the movement of larger rocks was caused by erosion of the loose material underneath them.

3.4. Subsurface borehole scanning and laboratory analysis

The presented data of this subsection was recorded at the salty plain of Laguna Santa Rosa, which is an about 1.6 km^2 large area, linked to Salar de Maricunga by a 100–500 m wide and about 12 km long elongated trench, mainly filled with evaporates. The surveyed area has a smooth, bright, salty surface with small undulations and polygonal ridges of 1–2 cm height. Liquid water coverage occurs at about 15–20% of this area at the southern edge, called Laguna Santa Rosa. Drilling was realized for sample acquisition to produce 3 cm in diameter and 20 cm deep holes.

The drilled and excavated material was inspected in a laboratory at the home institute using FTIR infrared spectroscopy for compositional analysis. The IR spectra are visible in Fig. 8 and Table 1. Based on FTIR ATR measurements the sample mainly consists of clay minerals, dominantly kaolinite (band positions: 1094 and 1003 cm^{-1}) and talc (872, 666 and 420 cm^{-1}), but there can be also palygorskite (1094 cm^{-1}),

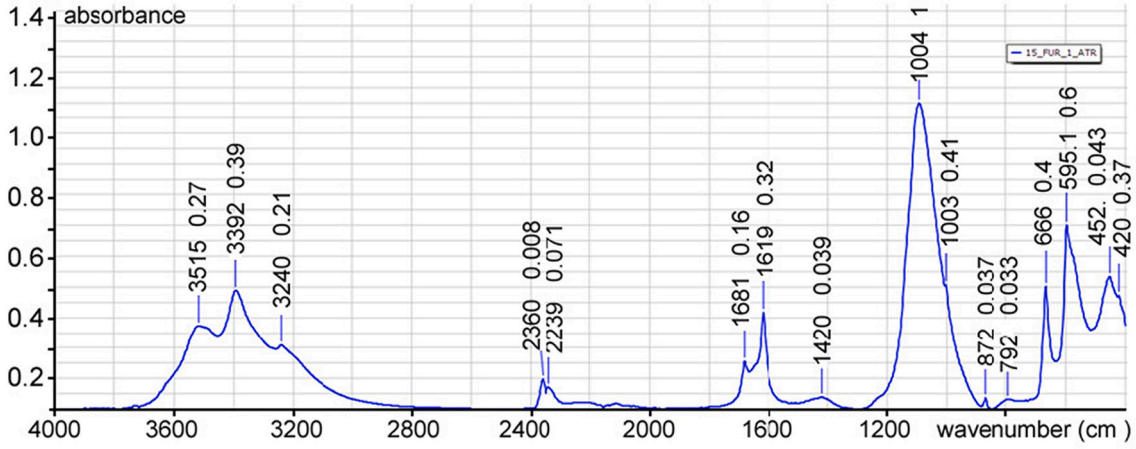

Fig. 8. Absorbance spectrum (4000–400 cm^{-1}) of the sample acquired from the borehole presented in Fig. 8 (id: 14 FUR).

Table 1
Summary of infrared peak positions and corresponding minerals in the sample. Please note that the 1–7 lines correspond to H_2O, CO_2 and OH partly from the laboratory atmosphere and partly embedded in the crystalline lattice.

Observed wavenumber (cm^{-1})	Absorbance	Mineral	Wavenumber according to references (cm^{-1})
3515.4	0.273		
3392.2	0.389		
3240.4	0.209		
2360.7	0.098	H_2O, OH, CO_2	
2339	0.071		
1681.3	0.156		
1619	0.317		
1420	0.039	carbonate (calcite, aragonite)	1420
1093.6	1.000	clay minerals (kaolinite, palygorskite, montmorillonite)/feldspar (plagioclase)	1095, 1100/1095, 1092
1003	0.410	kaolinite/vermikulite	1003/1004
871.7	0.037	talíc/illite	872/870
792.1	0.033	quartz	792
665.97	0.400	mica/talc	692–660/ 674–663
595.11	0.600	anhydrite/ gypsum	597–593/595
452.06	0.433	mica/quartz	465–440/454
420.4	0.370	talc	420

montmorillonite (1094 cm^{-1}), illite (872 cm^{-1}) or vermiculite (1003 cm^{-1}). In addition, it also contains feldspar (1095 cm^{-1}), mica (666 and 452 cm^{-1}), quartz (792, 452 cm^{-1}), carbonate minerals such as calcite or aragonite (1420 cm^{-1}) and gypsum or anhydrite (595 cm^{-1}). The Mars relevance of these minerals are discussed in the Discussion section.

The elevated salt content of the lakes in the region (often called lagunes) has a strong impact on the condensation of various salts by desiccation. Salt content measurements were realized in collected water samples at the home laboratory by measuring the electric conductivity of the water of two saline lakes (Laguna Santa Rosa, Laguna Verde), of a thermal spring and a small creek near Laguna Verde. The highest conductivity, 232 mS/cm was measured in the water of Laguna Verde, which in case of a NaCl solution would contribute to a concentration of more than 300 g/l (Williams and Sherwood, 1994). The water of the thermal spring and the small creek near Laguna Verde, as well as the water of Laguna Santa Rosa was characterized by lower conductivity values (between 3 and 8 mS/cm), similar to the conductivity of a 5 g/l NaCl solution. The conductivity of the permafrost thaw pond, lying at 5900 m above sea level was even lower, <1 mS/cm. The results show that the salinity of aquatic habitats in the region of Ojos del Salado varies on a broad scale from freshwater to brines close to saturation.

3.5. Occurrence of buried ice and snow

As the Ojos del Salado area is a dry, but also cold environment, the rare occurrence of subsurface snow and ice there is highly relevant for Mars. The following observations were indicated the existence of subsurface snow or ice: 1. direct observation of outcrops with buried ice (example in Fig. 9: near to Tejos camp at 5830 m altitude, where a small ephemeral creek outcrops the ice), 2. thermo- or natural cryokarstic depressions, 3. melt produced water runoff features, 4. outcrops from cross section following trenching and drills. The structure of the subsurface ice occurrence varies, including homogeneous and fine layer masses, while occasionally snow and partly compacted firn arise together. Snow or firn are usually buried by aeolian or mass wasting produced granular sediments. The following different types of solid H_2O occurrences could be identified in the subsurface:

- Buried snow below aeolian or mass movement produced debris cover, usually around 5000–6200 m elevation (Fig. 9 and 10).

Fig. 9. Outcrop of buried ice near to Tejos camp at 5850 m elevation (top). The ice is located at the bottom of a valley where melting from a nearby firn area pours its melted water here. The layering is produced by the incorporation of grains transported by wind and water, occasionally together with frozen ice. The cycles are produced by daily and annual temperature changes. Below an annotated version is also present without the person for scale.

- Pore ice above 5300 m between grains as a cementing material is present and poorly visible in the (usually trenching produced) outcrops, except where the cemented grains produced layers, are prepared by the selective erosion. The pore ice is probably formed by melting, percolation and freezing of surface precipitated snow produced water.
- Buried water ice from refrozen melt water, which is present in the subsurface at 5000–6500 m elevation, might occasionally form similar features such as pore ice.
- Buried firn with 0.6–0.7 g/cm^3 density as a homogeneous material is present with up to 10–20 cm thickness (occasionally with several separated layers on the top of each other), compacted probably by the overburden mass (aeolian sediments) in the 5200–6500 m elevation range.
- Buried glacier ice: compacted ice masses near remnant glacier bodies around 6300–6500 m elevation that are covered with slope debris.

The above listed occurrence types show a range of different solid H_2O between basically two end member types: the very shallow near surfaced buried porous H_2O, and the deeper located solid ice. Further details on the second one, including various permafrost features, are discussed in Nagy et al. (2019 and 2020).

Mars relevant, subsurface ice related degradational features are present as various depressions in the region, where the ice melted or sublimated away and the surface slumped (Eberhard and Sharples, 2013). A characteristic example is visible in Fig. 11 to demonstrate the active H_2O deposition/erosion cycles at 5200 m altitude. A layer of seasonal snow accumulated in the lee side of the 10–15 m high side-moraine what is visible in the right side of the images. This became

Fig. 10. Trenching produced ice outcrop at a 10–15 m high moraine side, where aeolian transported material deposited in the wind protected locations (27 03′41.13″ S 68 32′57.23″ W, 5250 m). The deposit covered the remnant snow and produced some compaction, forming firn-like layers at the bottom, with a porous snow like structure at the upper sections.

covered by aeolian and mass movement produced pumice-sand-dust layer in 2016, which was eroded away by 2018, then similar cycle happened again in 2019 and 2020, indicating that sedimentation occasionally could happen at the same preferred site and later exhumation could also happen again, repeatedly.

An additional example of the specific and fast surface modification can be seen in Fig. 12 at a trenching produced outcrop of typical local deposits. The snow, that transformed to a firn-like material, fell around 2 years before the photograph was taken, filling the depression. After that snow and dust-sand-pumice strata accumulated as a layered structure on the top of it with around 1 m thickness. There was no melting period after the first snow accumulation, and a second snow accumulation event took place, producing another around 1 m thick snow pack at the top of the layered grain section. The arrow marks an interbedded sand layer in the lower snow mass, demonstrating that, both materials were transported and deposited during the same period probably by the wind activity, but not simultaneously. It is worth to mention that ~100 mm of rain/precipitation being equivalent to ~1 m of snow (near 0 °C), however wind transport could accumulate a thick frost pack from moderately small average precipitation. This later got heavily dissected by sublimation, forming the so-called penitent-like structures or penitents here (Hargitai and Kereszturi, 2015), visible in the upper section of the image.

4. Discussion

During the field work at Ojos del Salado in the last years, several unique results emerged, as no other Mars analogue research project has targeted such a high altitude site before. This section is structured along the following subtopics: 1. discussion of the results in the order of the aeolian features, related surface modifications, examples on surface and shallow subsurface compositional and deeper subsurface ice related aspects; 2. relevance for Mars; 3. future perspectives related to the further exploration of this site. Although the site is rich in observational possibilities, the field work is hard and slow there because of the physiological consequences of the high altitude. As a result, some topics (like laboratory mineral analysis and aeolian transported grain analysis) could not provide such detailed results as would have been expected from a two weeks long expedition – however these data are worth presenting, as they provide a better context for this unique site.

4.1. Aeolian features: from grain size to ripples

The aeolian features found at Ojos del Salado contain mostly rough surface and poorly rounded volcanic grains, which because of the lack of cementation and dryness, strongly interact with the wind and show high mobility. The frequent idiomorph and euhedral shapes of grains point to that their source is relatively close and the grains did not suffer long distance transport to reach a mature shape – which is natural, given the hilly terrain. On Mars basaltic and basalt based weathered products (Chojnacki et al., 2014; Fenton et al., 2019) are abundant, thus the felsic material at Ojos del Salado differs from this. The lower density materials may better approximate the lower gravity environment on Mars and may represent a better analogue for the "density of the material/fluid" ratio. Based on the work of Zimbleman, 2008 particle size alone may not be the sole determining factor for why some ripples greatly exceed the size that is typical for similar features both on the Earth and Mars.

Grain size estimations for Mars, based on thermal inertia measurements, suggested the presence of 100–500 μm grains (Edgett and Christensen, 1991) in dunes. Nearby imaging of ripples at the Namib dunes on Mars by Curiosity suggests the same size range (Lapotre et al., 2018). In the case of mobile sand grains up to 0.5–2.5 mm (Baker et al., 2017) was observed on Mars. At the Bagnold dune field sand showed rounded to subrounded shape and fine to medium sizes (45–500 μm), with a few silt-sized or smaller grains with mainly crystalline and small amorphous components (Ehlmann et al., 2017; Edwards et al., 2018). Bimodal size distribution was also observed on Mars (Weitz et al., 2006), just like here, what might come from local boundary conditions such as sediment sources and wind conditions. Based on the trapped aeolian grains at Ojos del Salado, their size ranged between 10 and 1500 μm with a bimodal distribution as well, composed of a more populated peak (10–500 μm with probably even more grains from the lower size limit) and a usually smaller peak between 800 and 1500 μm. While quartz based grain analysis and detailed evaluation of grain maturity is established using Earth based examples, on Mars due to the specific conditions, the evaluation of maturity of grains requires further work (Cornwall et al., 2015; Kapui et al., 2021), partly because of the probable limited fluvial activity in space and time. The higher fragility of non-quartz based transported grains also contributes here, thus extrapolation to paleo-climatic conditions based on such transported grains is difficult, however the clarification of these aspects could be supported at such analogue sites.

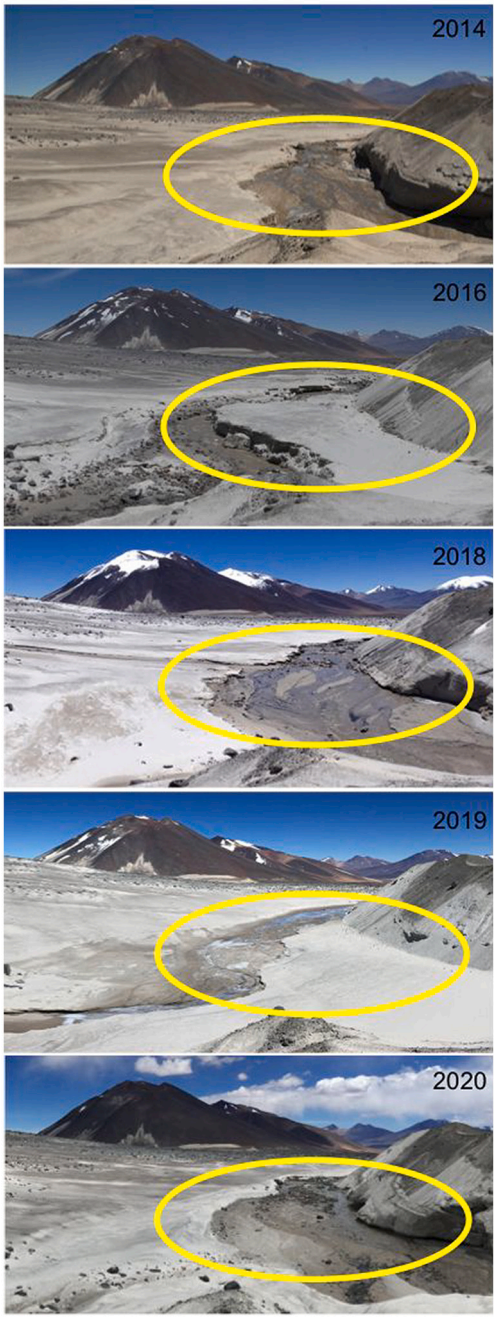

Fig. 11. Sequence of changes during 2014, 2016, 2018, 2019 and 2020 period (see the circled area), all images were recorded during local summer. First the snow deposited, then it got covered by slope mass movement debris and aeolian grains (2016), then it was degraded by meltwater system in 2018, covered again in 2019, and exhume by water flow again in 2020.

Since there are several uncertainties related to the formation and migration of ripples on Mars (Lapôtre et al., 2019; Sullivan et al., 2020), further field studies should be done here. Several ripples were identified by Opportunity rover at Meridiani Planum (Jerolmack et al., 2006) where they exhibit spatial grain size sorting with well-sorted coarse--grains at the crests and poorly sorted finer-grained in troughs. Earth based migration rate was found to be around meter / Earth year (Banks et al., 2018; Chojnacki et al., 2019). The vertical stratigraphy observed here at Ojos del Salado partly resembles to those on Mars, named gravel mantled dunes, both might be related to vibration induced movement (Bridges et al., 2015). Sand plus silt could produce bedforms through infiltration between larger grains, and support the relative uplift of the gravel. The conditions for the realization of this process could be surveyed at Ojos del Salado too, where heavier (denser) grains are occasionally present at the top of ripples, however the roughly similar size of higher and lower density grains makes it less probable that the vertical separation have been caused by vibration. Strong wind was observed at the 3- and 10-cm-high granule ripples at Great Sand Dunes National Park (Zimbelman et al., 2009), indicating that the winds, which are necessary to initiate migration, might be faster, than previously suggested. The field site presented in this work supports the clarification and further measurement of this candidate processes related to aeolian activity, where slope winds might also contribute. The flattening effect of very strong winds on ripples (Isenberg et al., 2011) could be also observed here in the future.

Although fine sand and coarse silt are present at Ojos del Salado, the general lack of even finer grains could be related to the strong wind activity that transports fine silt and clay sized grains in suspension away from the site at a faster rate than they are produced. The main method of transportation may be saltation for most of the measured grains, as they got trapped in all pockets even up to 0.5 m above the ground in the collectors. The similar size distribution of grains in most pockets suggests that the transport process was almost homogeneous regarding the carried mass up to 50 cm height above the ground.

However observations show that the larger grains might be more abundant at trap pockets located higher above the ground in some cases, which is incompatible with this model. One possible explanation is that if in the cold wintertime snow is accumulated at the location of wind traps, the local surface becomes elevated by this snow layer. During the harsh winter even stronger winds could be present than in summer, and they could carry larger grains, causing the unusual size distribution. The possible reason to emerge these larger grans only in the upper pockets might be a hypothetic snow layer present only wintertime, what inhibits the grain collection at the lower pockets. More field data is necessary to prove or disprove this hypothesis.

4.2. *Mars relevant surface changes*

Surface change monitoring on Mars is important and has been realized for aeolian and icy landforms. Orbital observations showed albedo changes after dust storms, by shifting albedo boundaries between surface units of different brightness (Geissler et al., 2016). Changes in the Endeavour crater showed that dome dunes persistently deflate, producing dark sand features across lighter regolith (Chojnacki et al., 2015). Additionally, aeolian processes might contribute to the episodic decrease of albedo and measured migration rates about several m per Earth year (Chojnacki et al., 2015), however there were diversity among the values including anomalous high migration rates. Based on in-situ observations, Curiosity has identified movement of large grains on freshly exposed surfaces, secondary grain flows on the slip face of Namib Dune, and a slump on a freshly exposed surface of a large ripple (Bridges et al., 2017). Various observations show, that considering all of the already observed annual changes on Mars, beside the seasonal surface elevation change in polar regions. While wind related changes for the surface of Mars considered mainly regarding the albedo modification, other changes could happen, including the already observe dune changes, vertical changes on Mars by infill and erosion of dust.

The surface change monitoring in the Ojos region revealed substantial modifications in the vertical heights in subsequent years surveying the site only during the local summer, e.g. January and February, mainly by the change of the areal distribution of dust, sand and pumice. This effect modifies the appearance of the area through the albedo, similar to the changes that dust storms cause on Mars (Fenton et al., 2007; Geissler, 2005). Few wind speed measurements have been performed in the region, especially no regular monitoring happened above 4500 m elevation. Slope winds are not characteristic at Ojos del Salado, however the western winds from the Puna plateau blows through this region regularly. Based on personal field experience, strong

Fig. 12. Buried snow overlain by layered sand-pumice pocket with eroded penitent-like structured snow on the top (at 27 05′21.73″ S 68 32′12.44″ W, 5870 m). The arrow marks a partly interbedded sand-pumice layer inside the snow, suggesting sand accumulation processes from the same period.

enough winds to carry dust and silt fraction are frequent, could occur several afternoons in a week. Wind related surface features can be identified up to 6200 m elevation. For context it is worth to mention that at a location about 200 km distance, during the Veladero Project Meteorological Data (between 2000 and 2002) observed 100 km/h hourly maximum wind speed during about 1% of time (Milana, 2009).

At Ojos del Salado wind effects could fill meter scale depressions and produce substantial changes (see some examples in Fig. 7). Thus rocks need not necessarily move to change their observed numbers, as the deposit could easily bury rocks up to dm size or erode pits down to 1 m depth. This example underlines that wind alone (or especially together with occasional snow events) could produce even m scale vertical topography and related surface appearance changes by infilling the depressions, besides changing the albedo by moving the surface dust cover on Mars, also in theory.

Assuming similar scale changes on Mars, MOLA based data might not be enough to identify 10 cm scale height changes. MOLA data have vertical and horizontal spatial resolution about 200 and 3 m respectively (Kolb and Okubo, 2009). However focusing on the relative changes of elevation, comparison of neighbouring points might improve the vertical sensitivity several times, but still below what should be required to identify the same scale at Ojos area. According to HiRISE stereo images based DTMs, these values are roughly in the range of 0.25–2 m and 1–3 m respectively (Parker and Calef, 2016; Sutton et al., 2015). Beyond these aspects, artefacts could also influence the accuracy (Kirk et al., 2017). However, using the different time recorded image based identification of rocks hiding by dust cover and later emerging by wind driven exhumation, the scale of about 10 cm vertical change could be identified on subsequent images around larger rocks.

4.3. Evaporates and surface composition

Shallow subsurface observations might provide important insight into the local geological history with moderate effort, as it was presented recently for the Mars analogue sites at Ibn Battuta Centre in the Sahara (Kereszturi et al., 2018). The laboratory analysis of the acquired samples showed mainly water related alteration minerals including phyllosilicates, talc, carbonates and gypsum there. These are also typically alteration produced minerals on Mars, where phyllosilicates (Bibring et al., 2006), carbonates (Ehlmann et al., 2008), talc (Bishop et al., 2018) and gypsum (Wilson and Bish, 2011) are used as indicators of wet weathering in the past.

The components of this evaporate assemblage are expected to occur in a sedimentary basin under dry climate. There is a specific importance of the occurrence of mineral paragenesis. On Mars the joint occurrence of phyllosilicates and evaporates could be identified: at Columbia Hills, Gusev crater (Wang et al., 2006), by the MER Opportunity rover on the rim of Endeavour crater at Meridiani Planum (Arvidson et al., 2014), by the MSL Curiosity in Yellowknife Bay at Gale crater (Vaniman et al., 2014), and by MEX-OMEGA and MRO-CRISM in several further locations on Mars. Regional co-exposures of phyllosilicates with either carbonates (Ehlmann et al., 2008, 2012; Carter and Poulet, 2012), sulfates (Poulet et al., 2005; Wiseman et al., 2008; Hamilton et al., 2008; Murchie et al., 2009; Wray et al., 2009; Milliken et al., 2014), or chlorides (Murchie et al., 2009) were found at different locations, even the presence of sulfate-bearing materials underlying phyllosilicate-bearing strata (Wray et al., 2010) were identified. The specific example of Ojos del Salado points to some important aspects that should be considered during the in-situ analysis of evaporates on Mars, for the

identification and separation of certain minerals. Feldspars (intact magmatic minerals) and phyllosilicates (weathering products) both present a major band around 1094–1095 cm^{-1}, but phyllosilicates also show bands at 1003, 872, 666 and 420 cm^{-1}. Kaolinite, paligorskite and montmorillonte (identified on Mars by remote sensing) all show a major band at 1094 cm^{-1}, although the separation of kaolinite was successful by another peak at 1003 cm^{-1}. Mica and phyllosilicates both present band at 666 cm^{-1}, the separation is supported by further bands of talc at 872 and 420 cm^{-1}. The hydrated state can be identified using the spectra between 1600 and 1700 cm^{-1}. Based on the above listed observations, a spectral resolution of around several cm^{-1} (~10) might be enough for the separation of components of a characteristic evaporate assemblage on the Earth, and potentially on Mars too using IR data. Complementary measurements would be useful for definite identification.

Regarding the shallow subsurface sampling, the composition is in agreement, that the site is an evaporite basin (dried up part of Laguna Verde), where previously water related weathered mineral alterations happened together with very fine grain sedimentation. Such a geologic setting seems to be Mars and astrobiology relevant, and could be used to infer formation conditions and even duration for active periods with a more detailed analysis in the future. As a result, the Ojos del Salado region could be an analogue field site that supports the better understanding of the geological history of ephemeral evaporative basins on Mars (Catling, 1999; Forsythe and Zimbelman, 1995; Irwin et al., 2015).

4.4. Subsurface ice occurrence

Beside the cryosphere at Ojos del Salado (discussed by Nagy et al., 2019), subsurface ice as almost pure H_2O with low contamination level from rocky debris, can be found in different forms. The degradation of subsurface ice and snow is suggested by the flowing meltwater originating from the subsurface, and outcrop walls of collapsed pits at the analysed region. Subsurface ice occurs in a variety of forms presented in section 3.6 above. In some cases the coverage formed in the last 1–3 years during the site monitoring (Fig. 7), demonstrating that the process is active and the buried snow formed under the current climatic regime despite the general dryness. The morphological observations also demonstrate that the signatures of the active process could be caught in the form of small (below m size) spatial resolution on-site images, where the vertical walls exposed subsurface settings to provide a simple way to identify the original structure. This is not necessarily observable form above and rarely (if similar sized) could have been identified by orbital images of Mars.

The occurrence of subsurface ice at Ojos del Salado is important as it contributes to the formation of depressions, partly similar to those on Mars, that are supposed to be produced by sublimation instead of melting (e.g. cryokarst, Head et al., 2011). Despite this, there are melting signatures on Mars too, produced by subsurface stored ice masses (Costard et al., 2002). The analogues at Ojos del Salado are useful in four aspects: 1. The connection between surface structures and the existence of subsurface ices could be analysed as occasionally natural outcrops are present. Trenching produced outcrops could also be made, thus they support as “ground truth” for resembling features on Mars. 2. They provide quantifiable surface structures where the volume of the missing ice could be roughly estimated. 3. The active annual surface changes could be monitored, and they support model calculations on subsurface melting (see some related calculations in Nagy et al., 2019. 4. On Mars, the depressions without connected flow related surface structures thought to be formed mainly by sublimation without melting. The Ojos site indicates however that melting might also arise without observable flow-features in the close vicinity (see the Fig. 11 in the Nagy et al., 2019), partly by percolation to the subsurface.

Based on the occurrence types of subsurface ices, a wide range of occurrence exists with different depth, density and formation methods – as a result it is expected that the Martian case might also be more difficult than the general view of having cryosphere and shallow buried snow. An important aspect is that various thermokarstic or cryokarstic features could be formed at Ojos del Salado from the simple setting of loose dust covered porous snow, and not necessarily in densely packed ice or permafrost. While several degradational features on Mars like cryokarstic depressions are thought to be analogous with permafrost degradational features like alases on the Earth, but in reality many of them might formed with the help of simple loose, poorly compacted snow without ice. This latter possibility should be better considered for Mars.

4.5. Mars relevant aspects

Based on the various results presented above, the Ojos del Salado region holds important data and observational possibility for the future as are listed in Table 2. Beside the separately listed topics, the interactions between them could be also the target of future analysis, especially the relation between surface temperature and humidity conditions, between subsurface temperature and ice storage, evaporate accumulation and desiccation, interaction of wind transported grains and snow burial for potential later melting and runoff. All of these are important Mars relevant topics (Diniega et al., 2021; Dundas et al., 2021). The connection and interaction between the observed large daily temperature fluctuation, the general dryness and the porous, loose material covered terrain are ideal for understanding the role of specific surface weathering and transport of the somewhat loose or partly cemented Martian regolith. The high elevation and mountainous environment produced not only low atmospheric pressure here, but also highly changeable conditions that increase the wind speed occasionally.

At the Ojos del Salado region evaporites, volcanic materials, the mobilization by fluvial, aeolian and glacial/periglacial transport processes under dry and cold conditions could be analysed. The joint occurrence of phyllosilicates, talc, gypsum and anhydrite suggests a moderately wet environment with potential signatures of drying processes and water loss from gypsum, producing anhydrite. Similar observations are expected in the dried up basins on Mars.

4.6. Logistical aspects

The presented site is accessible by regular four wheel drive cars and pickup trucks, with approximately 5–6 h driving from the nearest airport in Copiapo. Research work at the site is recommended during the local summer (January to March), because of the very low temperatures and strong winds in winter. Specific adaptation to working under reduced atmospheric pressure requires preparation and facilities, especially above altitude about 5000 m. The restrictions related to environmental protections are not as strict as for example in Svalbard (Steele et al., 2010) or Iceland (Ehlmann et al., 2012) or Antarctica (Dickinson and Rosen, 2003). Sampling is allowed without special authorization except for natural reserves there.

4.7. Future perspective

Compared to other Mars analogue sites, the Ojos del Salado region provides several complementary and unique possibilities for research (Kereszturi et al., 2020a, 2020b). UV irradiation is rarely considered as an important factor at Mars analogue sites, because most of them on the Earth are located at much lower altitudes. Here this unique characteristic could be exploited, for extremophile adaptation and rock weathering. On Mars the strong UV limits organic material survival on the surface (Laurent et al., 2019) where perchlorates together with UV radiation make the situation even worse (Wadsworth and Cockell, 2017). Shielding against UV radiation could be done by minerals or even ferric iron rich solutions (Gómez et al., 2007), resemble to clay-bearing Atacama soils provided shielding for organics (Ertem et al., 2017). Evaporates are helpful in this aspect as they let radiation penetrate to be useful for photosynthesis, while shielding against harmful UV light

Table 2
Mars relevant research topics that could be analysed at the Ojos del Salado region.

Topic	Specific local conditions	Target of analogue research	Corresponding Martian features, characteristics
surface evolution under dry and cold conditions in general	role of large temperature fluctuation and wind driven regolith changes	resistance and age of surface regolith, rate of transport	dry and slowly weathered surface material, rarely ice cemented at shallow depth mainly at high altitude locations, mobility of dust and sand that could cover surface ice by strong winds (Sefton-Nash et al., 2014)
wind ripples	up to 1 m high, 20–40 m wide, 100–300 m long ripples on the surface with specific granular characteristics	identification of processes and characteristics of grain movement, and accumulation, role of non-spherical and porous volcanic grains	many volcanic grains produced ripples (Lapotre et al., 2016), usually in non-quartz composed granular material, under potentially active migration today (Silvestro et al., 2010)
ephemeral water flow features	liquid water flow only during daytime in summer	reason of melting, water sources and characteristics of activity	gullies (Christensen, 2003) and other potential recent liquid flow related surface features
stability of lakes	high altitude ponding of cryosphere melting produced waterand evaporation	role of melting and cryospheric insulation in lake formation; analysis of temporal stability by inflow / evaporation rate	observations indicate that ephemeral lakes were abundant (Cabrol and Grin, 1999) on Mars, however their characteristics are poorly known
extreme organisms	cold and dry tolerant organisms	analysis of habitats, including related methodological development (sampling), better understanding the access to nutrients	ice and ephemeral melting related potential habitability (McKay and Davis, 1991), Earth based experiences to orient development of future in-situ methods
role of UV in surface weathering	long term exposure of strong UV under dry and cold conditions	identification of specific mineral alteration in volcanic material	better understanding of weathering under very high UV irradiation and dryness
behaviour of cryosphere	buried ice and snow with degradational structures	understanding how sublimation-melting-wind exposure interact and contribute in surface evolution at a dry terrain	wide range of cold-climate landforms (Morgenstern et al., 2007, van Gasselt et al., 2007), but more information is necessary on how to approach using numerical way of their degradation and understanding the role of climates on layered deposit formations (Sefton-Nash et al., 2012)

(Rothschild, 1990; Marschall et al., 2012). The consequences of UV radiation was analysed during the High Lake Project in the Andes (HLP, Cabrol et al., 2010), that might be relevant to early Earth too (Berkner and Marshall, 1965). At the Ojos del Salado site the analysed lake is smaller and located at an even higher altitude, thus it is more exposed to local changes than the previously investigated Licancabur at 6000 m, which was the highest lake analysed in the HLP (Aszalós et al., 2020a, 2020b). At a similarly UV exposed site at Victoria Land, Antarctica, snow in the pits in dolerite rocks produced Fe-rich clays (Allen and Conca, 1991), while at the Three Sisters volcanic complex in Oregon (Scudder et al., 2016) amorphous phases might be influenced by UV irradiation. Rare basaltic blocks can be found, about 500 m to the south of Laguna Verde (Fig. 13) at Ojos del Salado. The larger (meter sized) rocks are expected to withstand long term exposure on their surface as wind driven debris could not easily cover them.

Occasionally snow could cover the area for a brief period even in summer (usually up to a couple of days), and due to the active wind and mass movements, debris could cover substantially large (100 m – km sized) areas and keep the snow there protected against sublimation for years. Local melting of small scale could be observable in summer (Kereszturi, 2020), producing active runoff or percolation to the subsurface and cryokarstic structure formation. Similar sinkholes on ice cemented dunes in the Victoria Valleys suggest melting or sublimation and denivation features inside dunes (McGowan and Neil, 2005). Unique snow precipitation during dune migration might also emerge there, as well as at Ojos de Salado where large amount of easily erodible debris at the otherwise dry regions support the process.

Characteristics of the subsurface cryosphere, including the behaviour of dry sub-zero temperature ground could be analysed effectively at Ojos del Salado as dry and ice cemented regions are present within 1–10 km scale distances (Nagy et al., 2020). A more detailed mapping would enable to identify the connection between subsurface properties and surface morphology. Models on subsurface evolution at dry and cold terrain with limited H_2O supply could be also improved here. A possibility of liquid water below the ice of the cryosphere cannot the excluded, because of the geothermal heat and the existence of hot springs in the region, partly similar as suggested for Mars (Stamenkovic et al., 2019) and observed recently (Lauro et al., 2020).

Interaction of strong winds with the non-cemented volcanic regolith surface produces an actively changing environment. This effect might be critical for the creation of sublimation inhibiting debris blanket on fresh surface snow, and also to expose buried ice. Without such an effect these snow patches could have been easily sublimate and the appearance of liquid water runoff would be much smaller and rare. Several locations on Mars hold buried snow deposits (Bramson et al., 2017), where a similar process could contribute to the storing of ice. Such analogue aspects could be also investigated for example in the McMurdo Dry Valleys of Antarctica (Heldmann et al., 2012). However the Ojos del Salado site is unique in the sense because of the occasional very strong winds and the easily transportable loose, porous volcanic regolith together, certain mass of snow (up to around m in thickness) could be covered during a short period of time and also could be exposed later to strong solar illumination (because of the low geographical latitude of this site) to support melting. The wind produced moderately rounded shaped and rough surface volcanic grains of different densities, creating ripples in the region. Wind produced surface features have been analysed at several Mars analogue locations including Mojave desert and Iceland (Greeley et al., 2002; Ukstins et al., 2017). While ripples on Earth are usually small (below meter scale, Lapotre et al., 2016), at Ojos del Salado relatively large ripples could be analysed, similar in size to those on Mars (Neely et al., 2014).

5. Conclusion

Interactions observed at a new potential Mars analogue site were characterized in this work at the Ojos del Salado volcano, at the high

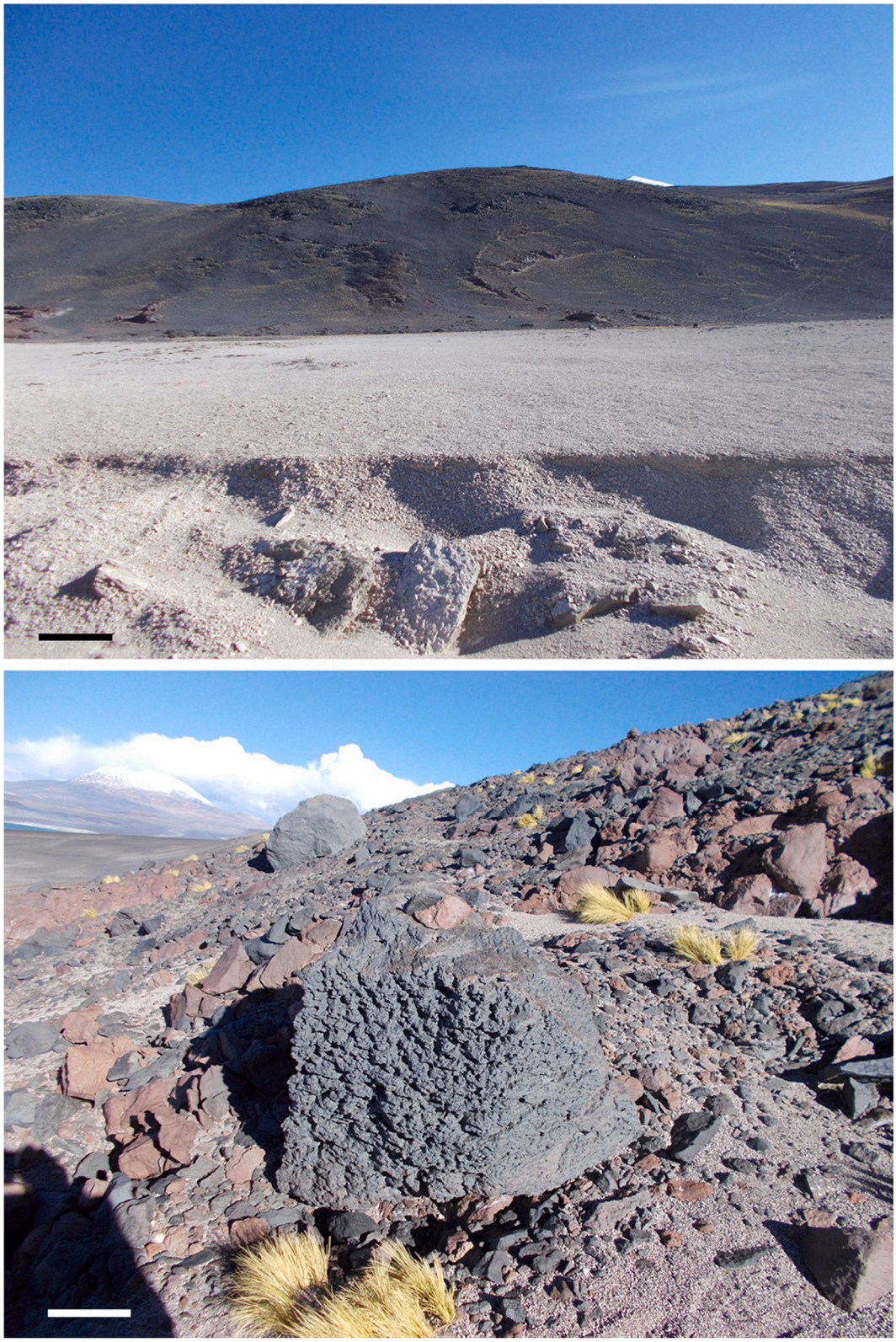

Fig. 13. Basaltic hillside close to the southern side of Laguna Verde. a: The dark slope in the distance (top), b: a roughly 1 m sized, heavily wind-chiseled basaltic rock on the slope of this hill in the middle of the image.

altitude area of the Atacama–Altiplano region. This site has a wide range of Mars relevant aspects, including the low average temperatures with large daily temperature variations, and frozen conditions in nighttime even during the summer. The general dryness with rare snow accumulation under the cold conditions influence the presence and occasionally the degradation of permafrost. The strong winds support surface modification, while the weathering is slow and influenced by strong UV radiation. Although the volcanic material is mostly evolved, basaltic rocks are also present there, and the porous structured tuffs could be used to understand the role of loose regolith in the geomorphology of Mars.

Snow masses could be accumulated mainly in winter up to meter thickness especially at areas protected from the wind and stored for year (s) long periods by fast debris burial at a very dry terrain, shielding it against sublimation. This Mars relevant interaction is active and fast in the area, contributing to the summertime melting of exhumed snow packs. The occasional snow and sand-dust accumulation and transport could effectively modify the surface topography. A similar process might be identified on Mars comparing subsequent HiRISE images. However the rarity of characteristic periglacial slope processes at the Ojos del Salado region is probably caused by the dry and water absorbing regolith and strong winds. Daily temperature and humidity cycling help to see the possibility of deliquescence and brine formation (Pal, 2021), providing insight to the process at different locations and periods, just like on Mars.

The wind driven grains composed of fine and coarse sand, with maximum sizes of around 200–400 μm. The collected aeolian material showed the same size distribution regardless of being collected from the ground or half meter above, demonstrating that the vertical transport was homogeneous in this layer. However in some cases the highest located traps showed a greater fraction of larger grains – the reason is still unknown but might be an episodic thick wintertime snow cover there during very strong wind activity. The UV driven weathering of volcanic rocks is a unique characteristic at the cold and dry environment, what also has an effect on the microbial community in the region.

This site provides most of those general analogue aspects like other sites on Earth, while its unique characteristics are the elevated UV radiation and the dryness together with ephemeral snow cover, the presence of permafrost and geothermal heat. It is accessible by cars up to 5200 m elevation for a low price compared to for example Svalbard or the Antarctic Dry Valleys. Because of the high altitude location, shorter than 2 weeks long expeditions are not suggested. The Ojos del Salado region should be considered as an important new Mars analogue site with many characteristics waiting for discovery.

Supplementary data to this article can be found online at https://doi.org/10.1016/j.icarus.2022.114941.

Declaration of Competing Interest

None.

Acknowledgement

The research work realized at the Ojos del Salado region was supported by the following projects and funds: The travel to the area was supported by the COOP_NN_116927 project, the drilling was supported by the ESA EXODRILTECH project, and the support from NKFIH for the Size and Shape Laboratory. Part of the field technology and facilities supported by the Hungarian Astronomical Non-profit Ltd. The logistical support is acknowledged from the *Földgömb az Expedíciós Kutatásért Alapítvány*, acknowledged from the Földgömb Foundation, and also from the helpful staff members of the Embassy of Hungary in Santiago, especially from Ambassador Ms. *V*erónica Chachin (Embassy of Chile in Hungary) and Ambassador Miklós Deák (Embassy of Hungary in Santiago de Chile). AI received funding from the European Research Council (ERC) under the European Union's Horizon 2020 research and innovation programme (Grant agreement No. 787263).

References

Ahumada, A.L., 2002. Periglacial phenomena in the high mountains of northwestern Argentina. South Afr. J. Sci. 98, 166–170.
Allen, C.C., Conca, J.-L., 1991. Weathering of basaltic rocks under cold, arid conditions - Antarctica and Mars. In: LPSC 21th, Proceedings, pp. 711–717.
Amashukeli, X., Grunthaner, F.J., Patrick, S.B., Yung, P.T., 2008. Subcritical water extractor for Mars analog soil analysis. Astrobiology 8, 597–604.
Ammann, C., Jenny, B., Kammer, K., Messerli, B., 2001. Late Quaternary glacier response to humidity changes in the arid Andes of Chile (18–29 S). Palaeog Palaecol. 172, 313–326.
Arvidson, R.E., Squyres, S.W., Bell, J.F., Catalano, J.G., Clark, B.C., Crumpler, L.S., de Souza, P.A., Fairén, A.G., Farrand, W.H., Fox, V.K., Gellert, R., Ghosh, A., Golombek, M.P., Grotzinger, J.P., Guinness, E.A., Herkenhoff, K.E., Jolliff, B.L., Knoll, A.H., Li, R., McLennan, S.M., Ming, D.W., Mittlefehldt, D.W., Moore, J.M., Morris, R.V., Murchie, S.L., Parker, T.J., Paulsen, G., Rice, J.W., Ruff, S.W., Smith, M. D., Wolff, M.J., 2014. Ancient aqueous environments at Endeavour crater Mars. Science 343 (6169), 1248097.
Aszalós, J.M., Szabó, A., Felföldi, T., Jurecska, L., Nagy, B., Borsodi, A.K., 2020a. Effects of active volcanism on bacterial communities in the highest altitude crater lake of Ojos del Salado (Dry Andes, Atacama). Astrobiology 20, 741–753.
Aszalós, J.M., Szabó, A., Megyes, M., Anda, D., Nagy, B., Borsodi, A.K., 2020b. Bacterial diversity of a high-altitude permafrost thaw pond located on Ojos del Salado (Dry-Andes, Atacama). Astrobiology 20, 754–765.
Azócar, G.F., Brenning, A., 2010. Hydrological and geomorphological significance of rock glaciers in the dry Andes, Chile (27–33 S). Permafr. Periglac. Process. 21, 42–53.
Azua-Bustos, A., Urrejola, C., Vicuña, R., 2012. Life at the dry edge: microorganisms of the Atacama Desert. FEBS Lett. 586 (18), 2939–2945.
Azua-Bustos, A., Caro-Lara, L., Vicuña, R., 2015. Discovery and microbial content of the driest site of the hyperarid Atacama Desert, Chile. Environ. Microbiol. Rep. 7 (3), 388–394.
Baker, V.R., 2001. Water and the Martian landscape. Nature 412, 228–236.
Baker, M., Lewis, K.W., Bridges, N., Newman, C., Van Beek, J., Lapotre, M., 2017. Aeolian transport of coarse sediment in the modern Martian environmentc. In: Dust in the Atmosphere of Mars abstract 6021.
Bakero, P.E., Gonzalez-Ferrand, O., Rex, C., 1987. Geology and geochemistry of the Ojos del Salado volcanic region, Chile. J. Geol. Soc. 144 (1), 85–96.
Banks, M.E., Fenton, L.K., Bridges, N.T., Geissler, P.E., Chojnacki, M., Runyon, K.D., Silvestro, S., Zimbelman, J.R., 2018. Patterns in mobility and modification of middle- and high-latitude Southern Hemisphere Dunes on Mars. J. Geophys. Res. Planet. https://doi.org/10.1029/2018JE005747.
Berkner, L.V., Marshall, L.C., 1965. On the origin and rise of oxygen concentration in the Earth attmonsphere. J. Atmos. Sci. 22 (3), 225–261.
Bibring, J.-P., Langevin, Y., Mustard, J.F., Poulet, F., Arvidson, R., Gendrin, A., Gondet, B., Mangold, N., Pinet, P., Forget, F., OMEGA Team, Berthé, M., Gomez, C., Jouglet, D., Soufflot, A., Vincendon, M., Combes, M., Drossart, P., Encrenaz, T., Fouchet, T., Merchiorri, R., Belluci, G.C., Altieri, F., Formisano, V., Capaccioni, F., Cerroni, P., Coradini, A., Fonti, S., Korablev, O., Kottsov, V., Ignatiev, N., Moroz, V., Titov, D., Zasova, L., Loiseau, D., Pinet, P., Doute, S., Schmitt, B., Sotin, C., Hauber, E., Hoffmann, H., Jaumann, R., Keller, U., Arvidson, R., Duxbury, T., Neukum, G., 2006. Global mineralogical and aqueous Mars history derived from OMEGA/Mars express data. Science 312, 400–404.
Bishop, J.L., Fairén, A.G., Michalski, J.R., Gago-Duport, L., Baker, L.L., Velbel, M.A., Gross, C., Rampe, E.B., 2018. Surface clay formation during short-term warmer and wetter conditions on a largely cold ancient Mars. Nat. Astron. 2, 206–213.
Blanco, Y., Rivas, L.A., Ruiz-Bermejo, M., Parro, V., 2013. Immunological detection of mellitic acid in the Atacama desert: implication for organics detection on Mars. Icarus 224, 326–333.
Blumthaler, M., Ambach, W., Ellinger, R., 1997. Increase in solar UV radiation with altitude. J. Photochem. Photobiol. B Biol. 39, 130–134.
Boy, D., Godoy, R., Guggenberger, G., Möller, R., Boy, J., 2017. Atacama Desert: Determination of two new extremophilic microbial model systems for space exploration and astrobiology studies - data from a large-scale transect study. In: 19th EGU abstract 18336.
Bramson, A.M., Byrne, S., Bapst, J., 2017. Preservation of Midlatitude Ice Sheets on Mars. J. Geophys. Res. 122, 2250–2266.
Bridges, N.T., Silva, S.L., Zimbleman, J.R., Loren, R.D., 2012. Formation conditions for coarse-grained megaripples on Earth and Mars from the Argentin Puna and wind tunnel experiments. In: 45th LPSC abstract 1855.
Bridges, N.T., Spagnuolo, M.G., de Silva, S.L., Zimbelman, J.R., Neely, E.M., 2015. Formation of gravel-mantled megaripples on Earth and Mars: insights from the Argentinean Puna and wind tunnel experiments. Aeolian Res. 17, 49–60.
Bridges, N.T., Sullivan, R., Newman, C.E., Navarro, S., van Beek, J., Ewing, R.C., Ayoub, F., Silvestro, S., Gasnault, O., Le Mouélic, S., Lapotre, M.G.A., Rapin, W., 2017. Martian aeolian activity at the Bagnold Dunes, Gale Crater: the view from the surface and orbit. J. Geophys. Res. 122, 2077–2110.
Cabrol, N.A., Grin, E.A., 1999. Distribution, classification, and ages of Martian Impact Crater Lakes. Icarus 142, 160–172.
Cabrol, N.A., Thomas, G., Witzke, B., 2001. Nomad rover field experiment, Atacama Desert, Chile 1. Science results overview. J. Geophys. Res. 106 (E4), 7785–7806.
Cabrol, N.A., Wettergreen, D., Warren-Rhodes, K., Grin, E.A., Moersch, J., Diaz, G.C., Cockell, C.S., Coppin, P., Demergasso, C., Dohm, J.M., Ernst, L., Fisher, G., Glasgow, J., Hardgrove, C., Hock, A.N., Jonak, D., Marinangeli, L., Minkley, E., Ori, G.G., Piatek, J., Pudenz, E., Smith, T., Stubbs, K., Thomas, Geb, Thompson, David, Waggoner, Alan, Wagner, Michael, Weinstein, Shmuel, Wyatt, Michael, 2007. Life in the Atacama: searching for life with rovers (science overview). J. Geophys. Res. 112 (G4). CiteID G04S02.
Cabrol, N.A., Grin, E.A., Chong-Diaz, G., Demergasso, C., HLP Team, 2010. The High Lakes Project/Shagan Initiative: Bridging Planets — From Mars to Earth and Back. Astrobiol Sci Conf 2010 abstract No. 1538, p. x05034.
Cabrol, N.A., Wettergreen, D.S., Warren Rhodes, K., Grin, E.A., Hare, T., Wei, J., Lambert, J., Moersch, J., Pointing, S., Tanaka, K., Tate, C., Thompson, D.R., Wagner, M., Wang, A., Zacny, K., 2014. Subsurface Life in the Atacama: Overview of the First Autonomous Traverse of a 1-m Rover-Mounted Drill. 45th LPSC abstract 1185.

Carter, J., Poulet, F., 2012. Orbital identification of clays and carbonates in Gusev crater. Icarus 219, 250–253.
Catling, D.C., 1999. A chemical model for evaporites on early Mars: possible sedimentary tracers of the early climate and implications for exploration. J. Geophys. Res. 104 (E7), 16453–16470.
Catling, D.C., Claire, M.W., Zahnle, K.J., Quinn, R.C., Clark, B.C., Hecht, M.H., Kounaves, S., 2010. Atmospheric origins of perchlorate on Mars and in the Atacama. J. Geophys. Res. 115. E00E11.
Chojnacki, M., Burr, D.M., Moersch, J.E., 2014. Valles Marineris dune fields as compared with other martian populations: diversity of dune compositions, morphologies, and thermophysical properties. Third Planet. Dunes Syst. 230, 96–142.
Chojnacki, M., Johnson, J.R., Moersch, J.E., Fenton, L.K., Michaels, T.I., Bell, J.F., 2015. Persistent aeolian activity at Endeavour crater, Meridiani Planum, Mars; new observations from orbit and the surface. Icarus 251, 275–290.
Chojnacki, M., Banks, M.E., Fenton, L.K., Urso, A.C., 2019. Boundary condition controls on the high-sand-flux regions of Mars. Geology. https://doi.org/10.1130/G45793.1.
Chojnacki, M., Vaz, D.A., Silvestro, S., Silva, D.C.A., 2021. Global heterogeneity of Martian Megaripples and transverse Aeolian Ridges: Distribution and activity. In: 52nd Lunar and Planetary Science Conference, Houston. Lunar and Planetary Institute p. Abstract #2524.
Christensen, P.R., 2003. Formation of recent martian gullies through melting of extensive water-rich snow deposits. Nature 422, 45–48.
Chubarova, N., Zhdanova, Y., Nezval, Y., 2016. A new parameterization of the UV irradiance altitude dependence for clear-sky conditions and its application in the on-line UV tool over Northern Eurasia. Atmos. Chem. Phys. 16, 11867–11881.
Clapperton, C.M., 1994. The Quaternary glaciation of Chile. Rev. Chil. Hist. Nat. 67, 369–383.
Cobos, D., Corte, A., 1990. Geocryological observations in Ojos del Salado, Central Andes, Lat. 27°. In: IGCP/UNESCO Project 297, 2nd Meeting, Geocryology of Southern Africa. Rhodes University, Grahamstown.
Cockell, C.S., 2002. The ultraviolet radiation environment of Earth and Mars: Past and present. In: Horneck, G., Baumstark-Khan, C. (Eds.), Astrobiology. Springer, Berlin, Heidelberg.
Cornwall, C., Bandfield, J.L., Titus, T.N., Schreiber, B.C., Montgomery, D.R., 2015. Physical abrasion of mafic minerals and basalt grains: application to martian aeolian deposits. Icarus 256, 13–21.
Costard, F., Forget, F., Mangold, N., Peulvast, J.P., 2002. Formation of recent Martian Debris flows by melting of near-surface ground ice at high obliquity. Science 295, 110–113.
Cousins, C.R., Crawford, I.A., Carrivick, J.L., Gunn, M., Harris, J., Kee, T.P., Karlsson, M., Carmody, L., Cockell, C., Herschy, B., Joy, K.H., 2013. Glaciovolcanic hydrothermal environments in Iceland and implications for their detection on Mars. J. Volcanol. Geotherm. Res. 256, 61–77.
Davila, A.F., Duport, L.G., Melchiorri, R., Jänchen, J., Valea, S., de los Rios, A., Fairén, A. G., Möhlmann, D., McKay, C.P., Ascaso, C., Wierzchos, J., 2010. Hygroscopic salts and the potential for life on Mars. Astrobiology 10, 617–628.
DeSilva, S.L., Francis, P.W., 1991. Volcanoes of the Central Andes. Springer, Berlin Heidelberg.
Dickinson, W.W., Rosen, M.R., 2003. Antarctic permafrost: an analogue for water and diagenetic minerals on Mars. Geology 31, 199–202.
Diniega, S., Bramson, A.M., Buratti, B., Buhler, P., Burr, D.M., Chojnacki, M., Conway, S. J., Dundas, C.M., Hansen, C.J., McEwen, A.S., Lapôtre, M.G.A., Levy, J., Mc Keown, L., Piqueux, S., Portyankina, G., Swann, C., Titus, T.N., Widmer, J.M., 2021. Modern Mars' geomorphological activity, driven by wind, frost, and gravity. Geomorphology 380 id. 107627.
Douglas, T.A., Mellon, M.T., 2019. Sublimation of terrestrial permafrost and the implications for ice-loss processes on Mars. Nat. Commun. 10 id. 1716.
Dundas, C.M., Becerra, P., Byrne, S., Chojnacki, M., Daubar, I.J., Diniega, S., Hansen, C. J., Herkenhoff, K.E., Landis, M.E., McEwen, A.S., Portyankina, G., Valantinas, A., 2021. Active Mars: a dynamic world. J. Geophys. Res. Planet 126 id. e06876.
Eberhard, R., Sharples, C., 2013. Appropriate terminology for karst-like phenomena: the problem with 'pseudokarst'. Int. J. Speleol. 42, 109–113.
Edgett, K.S., Christensen, P.R., 1991. The particle size of Martian aeolian dunes. J. Geophys. Res. 96, 22765–22776.
Edwards, C.S., Piqueux, S., Hamilton, V.E., Fergason, R.L., Herkenhoff, K.E., Vasavada, A.R., Bennett, K.A., Sacks, L., Lewis, K., Smith, M.D., 2018. The thermophysical properties of the Bagnold Dunes, Mars: ground-truthing orbital data. J. Geophys. Res. Planet 123, 1307–1326.
Ehlmann, B.L., Mustard, J.F., Murchie, S.L., Poulet, F., Bishop, J.L., Brown, A.J., Calvin, W.M., Clark, R.N., Des Marais, D.J., Milliken, R.E., Roach, L.H., Roush, T.L., Swayze, G.A., Wray, J.J., 2008. Orbital identification of carbonate-bearing rocks on Mars. Science 322, 1828.
Ehlmann, B.L., Bish, D.L., Ruff, S.W., Mustard, J.F., 2012. Mineralogy and chemistry of altered Icelandic basalts: application to clay mineral detection and understanding aqueous environments on Mars. J. Geophys. Res. 117 (E11), E004156.
Ehlmann, B.L., Edgett, K.S., Sutter, B., Achilles, C.N., Litvak, M.L., Lapotre, M.G.A., Sullivan, R., Fraeman, A.A., Arvidson, R.E., Blake, D.F., Bridges, N.T., Conrad, P.G., Cousin, A., Downs, R.T., Gabriel, T.S.J., Gellert, R., Hamilton, V.E., Hardgrove, C., Johnson, J.R., Kuhn, S., Mahaffy, P.R., Maurice, S., McHenry, M., Meslin, P.-Y., Ming, D.W., Minitti, M.E., Morookian, J.M., Morris, R.V., O'Connell-Cooper, C.D., Pinet, P.C., Rowland, S.K., Schröder, S., Siebach, K.L., Stein, N.T., Thompson, L.M., Vaniman, D.T., Vasavada, A.R., Wellington, D.F., Wiens, R.C., Yen, A.S., 2017. Chemistry, mineralogy, and grain properties at Namib and High dunes, Bagnold dune field, Gale crater, Mars: a synthesis of Curiosity rover observations. J. Geophys. Res. 122, 2510–2543.
Ertem, G., Ertem, M.C., McKay, C.P., Hazen, R.M., 2017. Shielding biomolecules from effects of radiation by Mars analogue minerals and soils. Int. J. Astrobiol. 16, 280–285.
Ettahri, M.A., Hargitai, H., 2020. Investigating discontinious channel systems on Mars and their possible terrestrial analogs. In: 51st Lunar and Planetary Science Conference (abstract 2728).
Ewing, S.A., Sutter, B., Owen, J., Nishiizumi, K., Sharp, W., Cliff, S.S., Perry, K., Dietrich, W., McKay, C.P., Amundson, R., 2006. A threshold in soil formation at Earth's arid hyperarid transition. Geochim. Cosmochim. Acta 70, 5293–5322.
Ewing, S.A., Macalady, J.L., Warren-Rhodes, K., McKay, C.P., Amundson, R., 2008. Changes in the soil C cycle at the arid-hyperarid transition in the Atacama Desert. J. Geophys. Res. 113 (G2). CiteID G02S90.
Lapotre, M.G.A., Ewing, R.C., Lamb, M.P., Fischer, W.W., Grotzinger, J.P., Rubin, D.M., Lewis, K.W., Ballard, M., Day, M.D., Gupta, S., Banham, S., Bridges, N., Des Marais, D.J., Fraeman, A.A., Grant, J.A., Ming, D.W., Mischna, M., Rice, M.S., Sumner, D.Y., Vasavada, A.R., Yingst, R.A., 2016. Origin of the two scales of wind ripples on Mars. In: AGU Fall Meeting abstract id. EP24A-02.
Fenton, L.K., Geissler, P.E., Haberle, R.M., 2007. Global warming and climate forcing by recent albedo changes on Mars. Nature 446, 646–649.
Fenton, L.K., Gullikson, A.L., Hayward, R.K., Charles, H., Titus, T.N., 2019. The Mars Global Digital Dune Database (MGD3): global patterns of mineral composition and bedform stability. Icarus 330, 189–203.
Fernández-Remolar, D.C., Chong-Díaz, G., Ruíz-Bermejo, M., Harir, M., Schmitt-Kopplin, P., Tziotis, D., Gómez-Ortíz, D., García-Villadangos, M., Martín-Redondo, M.P., Gómez, F., Rodríguez-Manfredi, J.A., Moreno-Paz, M., De Diego-Castilla, G., Echeverría, A., Urtuvia, V.N., Blanco, Y., Rivas, L., Izawa, M.R.M., Banerjee, N.R., Demergasso, C., Parro, V., 2013. Molecular preservation in halite- and perchlorate-rich hypersaline subsurface deposits in the Salar Grande basin (Atacama Desert, Chile): implications for the search for molecular biomarkers on Mars. J. Geophys. Res. 118, 922–939.
Flahaut, J., Martinot, M., Bishop, J.L., Davies, G.R., Potts, N.J., 2017. Remote sensing and in situ mineralogic survey of the Chilean salars: an analog to Mars evaporate deposits? Icarus 282, 152–173.
Forsythe, R.D., Zimbelman, J.R., 1995. A case for ancient evaporite basins on Mars. J. Geophys. Res. 100 (E3), 5553–5563.
Geissler, P.E., 2005. Three decades of Martian surface changes. J. Geophys. Res. 110 (E2). CiteID E02001.
Geissler, P.E., Fenton, L.K., Enga, M.-T., Mukherjee, P., 2016. Orbital monitoring of martian surface changes. Icarus 278, 279–300.
Gómez, F., Aguilera, A., Amils, R., 2007. Soluble ferric iron as an effective protective agent against UV radiation: implications for early life. Icarus 191, 352–359.
Gourronc, M., Bourgeois, O., Mège, D., Pochat, S., Bultel, B., Massé, M., Le Deit, L., Le Mouélic, S., Mercier, D., 2014. One million cubic kilometers of fossil ice in Valles Marineris: Relicts of a 3.5 Gy old glacial landsystem along the Martian equator. Geomorphology 204, 235–255.
Grau Galofre, A., Jellinek, A.M., Osinski, G.R., 2020. Valley formation on early Mars by subglacial and fluvial erosion. Nat. Geosci. 13 (10), 663–668.
Greeley, R., Bridges, N.T., Kuzmin, R.O., Laity, J.E., 2002. Terrestrial analogs to wind-related features at the Viking and Pathfinder landing sites on Mars. J. Geophys. Res. 107 (E1). CiteID 5005.
Groemer, G., Losiak, A., Soucek, A., Plank, C., Zanardini, L., Sejkora, N., Sams, S., 2016. The AMADEE-15 Mars simulation. Acta Astron. 129, 277–290.
Gurgurewicz, J., Mège, D., Carrère, V., Gaudin, A., Kostylew, J., Morizet, Y., Purcell, P. G., Le Deit, L., 2015. Inferring alteration conditions on Mars: insights from near-infrared spectra of terrestrial basalts altered in cold and hot arid environments. Planet Space Sci. 119, 137–154.
Hamilton, V.E., Morris, R.V., Gruener, J.E., Mertzman, S.A., 2008. Visible, near-infrared, and middle infrared spectroscopy of altered basaltic tephras: spectral signatures of phyllosilicates, sulfates, and other aqueous alteration products with application to the mineralogy of the Columbia Hills of Gusev Crater, Mars. J. Geophys. Res. 113 (E12), E12S43.
Hargitai, H., Kereszturi, A., 2015. Encyclopaedia of Planetary Landforms. Springer Publisher, New York, Heidelberg, Dordrecht, London.
Harrison, K.P., Grimm, R.E., 2005. Groundwater-controlled valley networks and the decline of surface runoff on early Mars. J. Geophys. Res. 110 (E12). E12S16.
Hauber, E., Ulrich, M., Reiss, D., Hiesinger, H., Balme, M.R., Gallagher, C.J., 2011. Towards climate reconstruction on Mars using landscape analysis: Insights from terrestrial analogues. In: AGU Fall Meeting abstract C54A-03.
Head, J.W., Mustard, J.F., Kreslavsky, M.A., Milliken, R.E., Marchant, D.R., Forget, F., Schon, S.C., Levy, J.S., 2011. Mars in the current glacial-interglacial cycle: exploring an anomalous period in Mars climate history. In: 42nd LPSC abstract 1315.
Heldmann, J.L., Conley, C.A., Brown, A.J., Fletcher, L., Bishop, J.L., McKay, C.P., 2010. Possible liquid water origin for Atacama Desert mudflow and recent gully deposits on Mars. Icarus 206, 685–690.
Heldmann, J.L., Marinova, M., Williams, K.E., Lacelle, D., Mckay, C.P., Davila, A., Pollard, W., Andersen, D.T., 2012. Formation and evolution of buried snowpack deposits in Pearse Valley, Antarctica, and implications for Mars. Antarct. Sci. 24 (3), 299–316.
Hock, A.N., Cabrol, N.A., Dohm, J.M., Piatek, J., Warren-Rhodes, K., Weinstein, S., Wettergreen, D.S., Grin, E.A., Moersch, J., Cockell, C.S., Coppin, P., Ernst, L., Fisher, G., Hardgrove, C., Marinangeli, L., Minkley, E., Ori, G.G., Waggoner, A., Wyatt, M., Smith, T., Thompson, D., Wagner, M., Jonak, D., Stubbs, K., Thomas, G., Pudenz, E., Glasgow, J., 2007. Life in the Atacama: a scoring system for habitability and the robotic exploration for life. J. Geophys. Res. 112 (G4), G04S08.
Houston, J., 2006. Variability of precipitation in the Atacama Desert: its causes and hydrological impact. Int. J. Climatol. 26, 2181–2198.

Houston, J., Hartley, A.J., 2003. The central Andean west-slope rainshadow and its potential contribution to the origin of hyper-aridity in the Atacama Desert. Int. J. Climatol. 23, 1453–1464.
Irwin, R.P., Tooth, S., Craddock, R.A., Howard, A.D., de Latour, A.B., 2014. Origin and development of theater-headed valleys in the Atacama Desert, northern Chile: morphological analogs to martian valley networks. Icarus 243, 296–310.
Irwin, R.P., Lewis, K.W., Howard, A.D., Grant, J.A., 2015. Paleohydrology of Eberswalde crater, Mars. Geomorphology 240, 83–101.
Isenberg, O., Yizhaq, H., Tsoar, H., Wenkart, R., Karnieli, A., Kok, J.F., Katra, I., 2011. Megaripple flattening due to strong winds. Geomorphology 131, 69–84.
Jerolmack, D.J., Mohrig, D., Grotzinger, J.P., Fike, D.A., Watters, W.A., 2006. Spatial grain size sorting in eolian ripples and estimation of wind conditions on planetary surfaces: application to Meridiani Planum, Mars. J. Geophys. Res. 111 (E12). CiteID E12S02.
Kapui, Zs., Kereszturi, A., Józsa, S., Király, Cs., Szalai, Z., 2021. Analysis of surface morphology of basaltic grains as environmental indicators for Mars. Planet. Space Sci. 208 https://doi.org/10.1016/j.pss.2021.105338.
Kereszturi, Á., 2020. Unique and potentially Mars-relevant flow regime and water sources at a high Andes-Atacama Site. Astrobiology 20, 723–740.
Kereszturi, A., Zs, Kapui, Ori, G.G., Taj-Eddine, K., Ujvari, G., 2018. Mars-relevant field experiences in Morocco: the importance of spatial scales and subsurface exploration. Astrobiology 18, 56–76.
Kereszturi, Á., Aszalós, J.M., Zs, Heiling, Ignéczi, Á., Zs, Kapui, Cs, Király, Sz, Leél-Össy, Nagy, B., Zs, Nemerkényi, Pál, B., Skultéti, Á., Szalai, Z., 2020a. Cold, dry, windy, and uv irradiated: surveying mars-relevant conditions in Ojos del Salado Volcano (Andes Mountains, Chile). Astrobiology 20, 677–683.
Kereszturi, A., Pal, B., Gyenis, A., 2020b. Temperature and humidity monitoring to identify ideal periods for liquefaction on Earth and Mars – data from the High Andes. Geol. Quarter. 64 (4) https://doi.org/10.7306/gq.1559.
Kirk, R.L., Howington-Kraus, E., Edmundson, K., Redding, B., Galuszka, D., Hare, T., Gwinner, K., 2017. Community tools for cartographic and photogrammetric processing of Mars express HRSC images. In: ISPRS Remote Sensing and Spatial Information Sciences, XLII-3/W1, pp. 69–76.
Kolb, K.J., Okubo, C.H., 2009. Coregistration of Mars Orbiter Laser Altimeter (MOLA) topography with high-resolution Mars images. Comput. Geosci. 35, 2304–2313.
Lapotre, M.G.A., Ewing, R.C., Weitz, C.M., Lewis, K.W., Lamb, M.P., Ehlmann, B.L., Rubin, D.M., 2018. Morphologic diversity of Martian Ripples: implications for large-ripple formation. Geophys. Res. Lett. 45, GL079029.
Lapôtre, M.G.A., Ielpi, A., Lamb, M.P., Williams, R.M.E., Knoll, A.H., 2019. Model for the formation of single-thread rivers in barren landscapes and implications for pre-Silurian and Martian fluvial deposits. J. Geophys. Res. - Earth Surf. 124 (12), 2757–2777.
Laurent, B., Cousins, C.R., Pereira, M.F.C., Martins, Z., 2019. Effects of UV-organic interaction and Martian conditions on the survivability of organics. Icarus 323, 33–39.
Lauro, S.E., Pettinelli, E., Caprarelli, G., Guallini, L., Rossi, A.P., Mattei, E., Cosciotti, B., Cicchetti, A., Soldovieri, F., Cartacci, M., Di Paolo, F., Noschese, R., Orosei, R., 2020. Multiple subglacial water bodies below the south pole of Mars unveiled by new MARSIS data. Nat. Astron. https://doi.org/10.1038/s41550-020-1200-6.
Levy, J.S., Head, J.W., Marchant, D.R., 2011. Geological Society, 354. Special Publications, London, pp. 167–182.
Marchant, D.R., Head, J.W., 2007. Antarctic Dry Valleys: microclimate zonation, variable geomorphic processes, and implications for assessing climate change on Mars. Icarus 192, 187–222.
Marschall, M., Dulai, S., Kereszturi, A., 2012. Migrating and UV screening subsurface zone on Mars as target for the analysis of photosynthetic life and astrobiology. Planet Space Sci. 71, 146–153.
Martin-Torres, F.J., Zorzano, M.-P., Valentin-Serrano, P., Harri, A.-M., Genzer, M., Kemppinen, O., Rivera-Valentin, E.G., Jun, I., Wray, J., Bo, Madsen M., Goetz, W., McEwen, A.S., Hardgrove, C., Renno, N., Chevrier, V.F., Mischna, M., Navarro-Gonzalez, R., Martinez-Frias, J., Conrad, P., McConnochie, T., Cockell, C., Berger, G., Vasavada, A., Sumner, D., Vaniman, D., 2015. Transient liquid water and water activity at gale crater on mars. Nat. Geosci. 8 (5), 357–361.
McGowan, H.A., Neil, D., 2005. Denivation Features of Polar Dunes: An Earth Analogue for Morphological Indicators of Solid Water on Mars. AGU Fall Meeting, abstract id. P13B-0145.
McKay, L., Claire, M., 2016. The presence and distribution of salts as a palaeoprecipitation proxy in atacama soils. In: EGU General Assembly id. EPSC2016-212.
McKay, C.P., Davis, W.L., 1991. Duration of liquid water habitats on early Mars. Icarus 90, 214–221.
McKay, C.P., Friedmann, E.I., Gómez-Silva, B., Cáceres-Villanueva, L., Andersen, D.T., Landheim, R., 2003. Temperature and moisture conditions for life in the extreme arid region of the Atacama Desert: four years of observations including the El Niño of 1997-1998. Astrobiology 3, 393–406.
McKay, C.P., Molaro, J.L., Marinova, M.M., 2009. High-frequency rock temperature data from hyper-arid desert environments in the Atacama and the Antarctic Dry Valleys and implications for rock weathering. Geomorphology 110, 182–187.
Mege, D., Hauber, E., De Craen, M., Moors, H., Minet, C., 2018. Discovery of a hydrothermal fissure in the Danakil depression. In: European Planetary Science Congress 2018 id.EPSC2018-381.
Milana, J.P., 2009. Largest wind ripples on the Earth? Geology 38, 219–220.
Milliken, R.E., Ewing, R.C., Fischer, W.W., Hurowitz, J., 2014. Wind-blown sandstones cemented by sulfate and clay minerals in Gale Crater, Mars. Geophys. Res. Lett. 41 (4), 1149–1154.
Moreno, T., Gibbons, W., 2007. The Geology of Chile. Geol Soc London, p. 414.
Morgenstern, A., Hauber, E., Reiss, D., van Gasselt, S., Grosse, G., Schirrmeister, L., 2007. Deposition and degradation of a volatile-rich layer in Utopia Planitia and implications for climate history on Mars. J. Geophys. Res. 112 (E6). CiteID E06010.
Mpodozis, C., Kay, S.M., Gardeweg, M., Coira, B., 1996. Geología de la región de Ojos del Salado (Andes centrales, 27°S): Implicancias de la migración hacia el este del frente volcánico Cenozoico Superior. In: 13° Congreso Geológico Argentino, Actas 3, 539-548, Buenos Aires.
Murchie, S.L., Mustard, J.F., Ehlmann, B.L., Milliken, R.E., Bishop, J.L., McKeown, N.K., Noe Dobrea, E.Z., Seelos, F.P., Buczkowski, D.L., Wiseman, S.M., Arvidson, R.E., Wray, J.J., Swayze, G., Clark, R.N., Des Marais, D.J., McEwen, A.S., Bibring, J.-P., 2009. A synthesis of Martian aqueous mineralogy after 1 Mars year of observations from the Mars Reconnaissance Orbiter. J. Geophys. Res. Planets 114 (E2), E00D06.
Nagy, B., Mari, L., Kovács, J., Zs, Nemerkényi, Zs, Heiling, 2014a. Környezetváltozás a SzárazAndokban: az Ojos del Salado monitoring vizsgálata. In: Cserny, T., Kovács-Pálffy, P., Krivánné Horváth, Á. (Eds.), HUNGEO 2014 Magyar Földtudományi szakemberek XII. találkozója: Magyar felfedezők és kutatók a természeti erőforrások hasznosításáért: cikkgyűjtemény. Budapest: Magyarhoni Földtani Társulat, pp. 53–62 (ISBN:978-963-8221-53-7).
Nagy, B., Mari, L., Kovács, J., Zs, Nemerkényi, Zs, Heiling, 2014b. Az Ojos del Salado monitoring vizsgálata: jég- és vízjelenlét a Föld legszárazabb magashegységében. In: Sansumné Molnár, J., Siskáné Szilasi, B., Dobos, E. (Eds.), VII. Magyar Földrajzi Konferencia kiadványa, Miskolc, pp. 449–459 (ISBN: 978-963-358-063-9).
Nagy, B., Ignéczi, A., Kovács, J., Szalai, Z., Lí, Mari, 2019. Shallow ground temperature measurements on the highest volcano of the Earth, the Mt. Ojos del Salado, Arid Andes, Chile. Permafrost Periglacial Proc. 30, 3–18.
Nagy, B., Kovács, J., Ignéczi, Á., Sz, Beleznai, Mari, L., Kereszturi, Á., Szalai, Z., 2020. The thermal behavior of ice-bearing ground: the highest cold, dry desert on Earth as an analog for conditions on Mars, at Ojos del Salado, Puna de Atacama-Altiplano Region. Astrobiology 20, 701–722.
Neely, E.M., Spagnuolo, M.G., de Silva, S.L., Bridges, N.T., Zimbelman, J.R., 2014. Methodology of Wind Tunnel Experiments Applied to Gravel Megaripple Formation on Earth and Mars. 45th LPSC abstract 1777.
Ori, G.G., Dell'Arciprete, I., Taj Eddine, K., 2014. The Activities of the Ibn Battuta Centre (Morocco) and the Sahara as Large-Scale Mars Analogue. In: 45th Lunar and Planetary Science Conference abstract 1898.
Óscar, G.F., 1995. Volcanes de Chile. Instituto Geográfico Militar Yearbook, Santiago, Chile, p. 640.
Oyarzun, C.G., 1987. Inventario de Glaciares de los Andes Chilenos desde los 180 a los 320 de Latitud Sur. Revista de Geografía Norte Grande 14, 35–48.
Pal, B., 2021. Global Deliquescence Possibility on Present Day Mars from Model Calculations. 52nd LPSC abstract 1864.
Pandey, S., Clarke, J., Nema, P., Bonaccorsi, R., Som, S., Sharma, M., Phartiyal, B., Rajamani, S., Mogul, R., Martin-Torres, J., Vaishampayan, P., Blank, J., Steller, L., Srivastava, A., Singh, R., McGuirk, S., Zorzano, M.-P., Güttler, J.M., Mendaza, T., Soria-Salinas, A.A.S., Ansari, A., Singh, V.K., Mungi, C., Bapat, N., 2020. Ladakh: diverse, high-altitude extreme environments for off-earth analogue and astrobiology research. Int. J. Astrobiol. 19, 78–98.
Parker, T., Calef, F.J., 2016. MSL Gale Merged Digital Elevation Model. Publisher: PDS Annex, U.S. Geological Survey. http://bit.ly/MSL_DEM.
Parro, V., de Diego-Castilla, G., Moreno-Paz, M., Blanco, Y., Cruz-Gil, P., Rodríguez-Manfredi, J.A., Fernández-Remolar, D., Gómez, F., Gómez, M.J., Rivas, L.A., Demergasso, C., Echeverría, A., Urtuvia, V.N., Ruiz-Bermejo, M., García-Villadangos, M., Postigo, M., Sánchez-Román, M., Chong-Díaz, G., Gómez-Elvira, J., 2011. A microbial oasis in the hypersaline Atacama subsurface discovered by a life detector chip: implications for the search for life on Mars. Astrobiology 11 (10), 969–996.
Peeters, Z., Quinn, R., Martins, Z., Sephton, M.A., Becker, L., van Loosdrecht, M.C.M., Brucato, J., Grunthaner, F., Ehrenfreund, P., 2009. Habitability on planetary surfaces: interdisciplinary preparation phase for future Mars missions. Int. J. Astrobiol. 8, 301–315.
Piatek, J.L., Hardgrove, C., Moersch, J.E., Drake, D.M., Wyatt, M.B., Rampey, M., Carlisle, O., Warren-Rhodes, K., Dohm, J.M., Hock, A.N., Cabrol, N.A., Wettergreen, D.S., Grin, E.A., Diaz, G.C., Coppin, P., Weinstein, S., Cockell, C.S., Marinangeli, L., Ori, G.G., Smith, T., Jonak, D., Wagner, M., Stubbs, K., Thomas, G., Pudenz, E., Glasgow, J., 2007. Surface and subsurface composition of the Life in the Atacama field sites from rover data and orbital image analysis. J. Geophys. Res. 112 (G4). CiteID G04S04.
Poulet, F., Bibring, J.-P., Mustard, J.F., Gendrin, A., Mangold, N., Langevin, Y., Arvidson, R.E., Gondet, B., Gomez, C., 2005. Phyllosilicates on Mars and implications for early martian climate. Nature 438, 623–627.
Preston, L., Grady, M., Barber, S., 2012. Concepts for Activities in the Field for Exploration: The Catalogue of Planetary Analogues. The Open University.
Pulschen, A.A., Rodrigues, F., Duarte, R.T., Araujo, G.G., Santiago, I.F., Paulino-Lima, I. G., Rosa, C.A., Kato, Massuo J., Pellizari, V.H., Galante, D., 2015. UV-resistant yeasts isolated from a high-altitude volcanic area on the Atacama Desert as eukaryotic models for astrobiology. Microbiol. Open 4, 574–588.
Ross, A., Kosmo, J., Janoiko, B., 2013. Historical synopses of desert RATS 1997-2010 and a preview of desert RATS 2011. Acta Astron. 90, 182–202.
Rothschild, L.J., 1990. Earth analogs for Martian life. Microbes in evaporites, a new model system for life on Mars. Icarus 88, 246–260.
Schmucki, D.A., Philipona, R., 2002. Ultraviolet radiation in the Alps: The altitude effect. In: Proceedings of SPIE - The International Society for Optical Engineering, 4482. https://doi.org/10.1117/12.452923.
Schulze-Makuch, D., Wagner, D., Kounaves, S.P., Mangelsdorf, K., Devine, K.G., de Vera, J.-P., Schmitt-Kopplin, P., Grossart, H.P., Parro, V., Kaupenjohann, M., Galy, A., Schneider, B., Airo, A., Frösler, J., Davila, A.F., Arens, F.L., Cáceres, L.,

Solís, C., Francisco, C.D., Dartnell, L., DiRuggiero, J., Flury, M., Ganzert, L., Gessner, M.O., Grathwohl, P., Guan, L., Heinz, Jacob, Hess, M., Keppler, F., Maus, D., McKay, C.P., Meckenstock, R.U., Montgomery, W.O., Elizabeth, A., Probst, Alexander J., Sáenz, Johan S., Sattler, Tobias, Schirmack, Janosch, Sephton, M.A., Schloter, M., Uhl, J., Valenzuela, B., Vestergaard, G., Wörmer, L., Zamorano, P., 2018. Transitory microbial habitat in the hyperarid Atacama Desert. PNAS 115, 2670–2675.

Schwendner, P., Cockell, C.S., MASE Team, 2018. Mars Analogues for Space Exploration — The MASE Project. LPSC 49th abstract 1648.

Scudder, N., Horgan, B.H.N., Rutledge, A.M., Rampe, E.B., 2016. Chemical Weathering on a Cold and Wet Ancient Mars: New Insights from a Glacial Mars Analog Site. AGU Fall Meeting (abstract id.P33D-2183).

Sefton-Nash, E., Catling, D.C., Wood, S.E., Grindrod, P.M., Teanby, N.A., 2012. Topographic, spectral and thermal inertia analysis of interior layered deposits in Iani Chaos, Mars. Icarus 221, 20–42.

Sefton-Nash, E., Teanby, N.A., Newman, C., Clancy, R.A., Richardson, M.I., 2014. Constraints on Mars' recent equatorial wind regimes from layered deposits and comparison with general circulation model results. Icarus 230, 81–95.

Silvestro, S., Fenton, L.K., Vaz, D.A., Bridges, N.T., Ori, G.G., 2010. Ripple migration and dune activity on Mars: evidence for dynamic wind processes. Geophys. Res. Lett. 37. CiteID L20203.

Skelley, Alison M., Aubrey, Andrew D., Willis, Peter A., Amashukeli, Xenia, Ehrenfreund, Pascale, Bada, Jeffrey L., Grunthaner, Frank J., Mathies, Richard A., 2007. Organic amine biomarker detection in the Yungay region of the Atacama Desert with the Urey instrument. J. Geophys. Res. 112 (G4). CiteID G04S11.

Smith, T., Thompson, D.R., Wettergreen, D.S., Cabrol, N.A., Warren-Rhodes, K.A., Weinstein, S.J., 2007. Life in the Atacama: Science autonomy for improving data quality. J. Geophys. Res. 112 (G4). CiteID G04S03.

Sobron, P., Lefebvre, C., Leveille, R., Koujelev, A., Haltigin, T., Du, H., Wang, A., Cabrol, N., Zacny, K., Craft, J., 2013. Geochemical profile of a layered outcrop in the Atacama analogue using laser-induced breakdown spectroscopy: implications for Curiosity investigations in Gale. Geophys. Res. Lett. 40, 1965–1970.

Spiga, A., Hinson, D.P., Madeleine, J.-B., Navarro, T., Millour, E., Forget, F., Montmessin, F., 2017. Snow precipitation on Mars driven by cloud-induced night-time convection. Nat. Geosci. 10 (9), 652–657.

Stalport, F., Glavin, D.P., Eigenbrode, J.L., Bish, D., Blake, D., Coll, P., Szopa, C., Buch, A., McAdam, A., Dworkin, J.P., Mahaffy, P.R., 2012. The influence of mineralogy on recovering organic acids from Mars analogue materials using the "one-pot" derivatization experiment on the Sample Analysis at Mars (SAM) instrument suite. Planet Space Sci. 67, 1–13.

Stamenkovic, V., Plesa, A.-C., Breuer, D., Mischna, M., 2019. Mars subsurface hydrology in 4D. In: 50th Lunar and Planetary Science Conferenc (abstract 2796).

Steele, A., Fries, M.D., Amundsen, H.E.F., Mysen, B.O., Fogel, M.L., Schweizer, M., Boctor, N.Z., 2010. Comprehensive imaging and Raman spectroscopy of carbonate globules from Martian meteorite ALH 84001 and a terrestrial analogue from Svalbard. Meteorit. Planet. Sci. 42, 1549–1566.

Sullivan, R., Bridges, N., Herkenhoff, K., Hamilton, V., Rubin, D., 2014. Ttransverse aeolian ridges (tars) as megaripples: Rover encounters at Meridiani Planum, Gusev, and Gale. In: Eighth International Conference on Mars, 2014, p. 1424.

Sullivan, R., Kok, J.F., Katra, I., Yizhaq, H., 2020. A broad continuum of Aeolian impact ripple morphologies on Mars is enabled by low wind dynamic pressures. J. Geophys. Res. Planet 125. https://doi.org/10.1029/2020JE006485.

Sutter, B., Dalton, J.B., Ewing, S.A., Amundson, R., McKay, C.P., 2007. Terrestrial analogs for interpretation of infrared spectra from the Martian surface and subsurface: sulfate, nitrate, carbonate, and phyllosilicate-bearing Atacama Desert soils. J. Geophys. Res. 112 (G4), G04S10.

Sutton, S.S., Chojnacki, M., Kilgallon, A., the HiRISE Team, 2015. Precision and accuracy of simultaneously collected HiRISE digital terrain models. In: 46th Lunar and Planetary Science Conference abstract 3010.

Thirsk, R., Williams, D., Anvari, M., 2007. NEEMO 7 undersea mission. Acta Astron. 60, 512–517.

Ukstins, I., Sara, M., Riishuus, M., Schmidt, M.E., Yingst, R.A., Berger, J., 2017. Insights from Askja sand sheet, Iceland, as a depositional analogue for the Bagnold Dune Field, Gale Crater, Mars. In: AGU Fall Meeting abstract #P31A-2789.

Valdivia-Silva, J.E., Navarro-González, R., McKay, C., 2009. Thermally evolved gas analysis (TEGA) of hyperarid soils doped with microorganisms from the Atacama Desert in southern Peru: implications for the Phoenix mission. Adv. Space Res. 44, 254–266.

van Gasselt, S., Hauber, E., Neukum, G., 2007. Cold-climate modification of Martian landscapes: a case study of a spatulate debris landform in the Hellas Montes Region, Mars. J. Geophys. Res. 112 (E9). CiteID E09006.

Vaniman, D.T., et al., 2014. Mineralogy of a Mudstone at Yellowknife Bay, Gale Crater, Mars. Science 343 (6169), 1243480.

Vitek, P., Jehlička, J., Edwards, H.G.M., Hutchinson, I., Ascaso, C., Wierzchos, J., 2014. Miniaturized Raman instrumentation detects carotenoids in Mars-analogue rocks from the Mojave and Atacama deserts. Phil. Trans. Roy Soc. A 372, 20140196–20140196.

Vuille, M., Ammann, C., 1997. Regional snowfall patterns in the high, arid Andes. In: Climatic Change at High Elevation Sites. Springer, Netherlands, pp. 181–191.

Wadsworth, J., Cockell, C.S., 2017. Perchlorates on Mars enhance the bacteriocidal effects of UV light. Sci. Rep. 7 id. 4662.

Wang, A., Korotev, R.L., Jolliff, B.L., Haskin, L.A., Crumpler, L., Farrand, W.H., Herkenhoff, K.E., de Souza, P., Kusack, A.G., Hurowitz, J.A., Tosca, N.J., 2006. Evidence of phyllosilicates in Wooly Patch, an altered rock encountered at West Spur, Columbia Hills, by the Spirit rover in Gusev crater, Mars. J. Geophys. Res. 111 https://doi.org/10.1029/2005JE002516. E02S16.

Warren-Rhodes, K., Weinstein, S., Dohm, J., Piatek, J., Minkley, E., Hock, A., Cockell, C., Pane, D., Ernst, L.A., Fisher, G., Emani, S., Waggoner, A.S., Cabrol, N.A., Wettergreen, D.S., Apostolopoulos, D., Coppin, P., Grin, E., Diaz, C., Moersch, J., Ori, G.G., Smith, T., Stubbs, K., Thomas, G., Wagner, M., Wyatt, M., 2007. Searching for microbial life remotely: satellite-to-rover habitat mapping in the Atacama Desert, Chile. J. Geophys. Res. 112 (G4). G04S05.

Warren-Rhodes, K., Lee, K., Archer, S., Lacap, D., Ng-Boyle, L., Wttergreen, D., Zacny, K., Demergasso, C., Moersch, J., Chong, G., Vijayarangan, S., Thebes, C., Wagner, M., Tanaka, K., Hare, T., Tate, C., Wang, A., Wei, J., Foil, G., Cabrol, N., Pointing, S., 2018. Soil microbial habitats in an extreme desert Mars-analogue environment. In: 2018. Soil Microbial Habitats in an Extreme Desert Mars-Analogue Environment in preparation.

Weidinger, T., Istenes, Z., Hargitai, H., Tepliczky, I., Bérczi, Sz, 2009. Micrometeorological Station at the Mars Analog Field Work, Utah, April, 2008. 40th LPSC abstract 1282.

Weitz, C.M., Anderson, R.C., Bell, J.F., Farrand, W.H., Herkenhoff, K.E., Johnson, J.R., Jolliff, B.L., Morris, R.V., Squyres, S.W., Sullivan, R.J., 2006. Soil grain analyses at Meridiani Planum, Mars. J. Geophys. Res. 111 (E12). CiteID E12S04.

Wierzchos, J., Ascaso, C., McKay, C.P., 2006. Endolithic Cyanobacteria in Halite Rocks from the hyperarid core of the Atacama Desert. Astrobiology 6, 415–422.

Wierzchos, J., de Los Ríos, A., Dávila, A.F., Cámara, B., Valea, S., Estevé, I., Solé, A., Roldán, M., Rodriguéz, R., Sánchez-Almazo, I.M., McKay, C.P., Ascaso, C., 2009. Primary producers in extreme arid environment of the Atacama Desert: where, how and when? Geochim. Cosmochim. Acta Suppl. 73, A1439.

Wierzchos, J., Davila, A.F., Sánchez-Almazo, I.M., Hajnos, M., Swieboda, R., Ascaso, C., 2012. Novel water source for endolithic life in the hyperarid core of the Atacama Desert. Biogeosci 9 (6), 2275–2286.

Wierzchos, J., Davila, A.F., Artieda, O., Cámara-Gallego, B., de los Ríos, A., Nealson, K. H., Valea, S., Teresa García-González, M., Ascaso, C., 2013. Ignimbrite as a substrate for endolithic life in the hyper-arid Atacama Desert: implications for the search for life on Mars. Icarus 224, 334–346.

Wilcox, A.C., Escauriaza, C., Agredano, R., Mignot, E., Zuazo, V., Otárola, S., Castro, L., Gironás, J., Cienfuegos, R., Mao, L., 2016. An integrated analysis of the March 2015 Atacama floods. Geophys. Res. Lett. 43, 8035–8043.

Williams, W.D., Sherwood, J.E., 1994. Definition and measurement of salinity in salt lakes. Int. J. Salt Lake Res. 3 (1), 53–63.

Wilson, S.A., Bish, D.L., 2011. Formation of gypsum and bassanite by cation exchange reactions in the absence of free-liquid H_2O: implications for Mars. J. Geophys. Res. 116 (E9). CiteID E09010.

Wiseman, S.M., Arvidson, R.E., Andrews-Hanna, J.C., Clark, R.N., Lanza, N.L., Des Marais, D., Marzo, G.A., Morris, R.V., Murchie, S.L., Newsom, H.E., Noe Dobrea, E. Z., Ollila, A.M., Poulet, F., Roush, T.L., Seelos, F.P., Swayze, G.A., 2008. Phyllosilicate and sulfate-hematite deposits within Miyamoto crater in southern Sinus Meridiani. Mars. Geophy. Res. Lett. 35 (19), L19204.

Wray, J.J., Noe Dobrea, E.Z., Arvidson, R.E., Wiseman, S.M., Squyres, S.W., McEwen, A. S., Mustard, J.F., Murchie, S.L., 2009. Phyllosilicates and sulfates at Endeavour Crater, Meridiani Planum, Mars. Geophys. Res. Lett. 36 (21), L21201.

Wray, J.J., Squyres, S.W, Roach, L.H., Bishop, J.L., Mustard, J.F., Noe Dobrea, E.Z., 2010. Identification of the Ca-sulfate bassanite in Mawrth Vallis, Mars. Icarus 209 (2), 416–421.

Zimbelman, J.R., Irwin, R.P., Williams, S.H., Bunch, F., Valdez, A., Stevens, S., 2009. The rate of granule ripple movement on Earth and Mars. Icarus 203, 71–76.

Zimbleman, J.R., 2008. The Transition Between Sand Ripples and Megaripples. American Geophysical Union, Fall Meeting 2018 abstract #EP43A-07.